Pd_nCO ($n = 1,2$): Accurate Ab Initio Bond Energies, Geometries, and Dipole Moments and the Applicability of Density Functional Theory for Fuel Cell Modeling

Nathan E. Schultz, Benjamin F. Gherman, Christopher J. Cramer, and Donald G. Truhlar*

Department of Chemistry and Supercomputing Institute, University of Minnesota, 207 Pleasant Street Southeast, Minneapolis, Minnesota 55455

Received: July 14, 2006; In Final Form: August 18, 2006

Electrode poisoning by CO is a major concern in fuel cells. As interest in applying computational methods to electrochemistry is increasing, it is important to understand the levels of theory required for reliable treatments of metal−CO interactions. In this paper we justify the use of relativistic effective core potentials for the treatment of PdCO and hence, by inference, for metal−CO interactions where the predominant bonding mechanism is charge transfer. We also sort out key issues involving basis sets and we recommend that bond energies of 17.2, 43.3, and 69.4 kcal/mol be used as the benchmark bond energy for dissociation of Pd_2 into Pd atoms, PdCO into Pd and CO, and Pd_2CO into Pd_2 and CO, respectively. We calculated the dipole moments of PdCO and Pd_2CO, and we recommend benchmark values of 2.49 and 2.81 D, respectively. Furthermore, we tested 27 density functionals for this system and found that only hybrid density functionals can qualitatively and quantitatively predict the nature of the σ-donation/π-back-donation mechanism that is associated with the Pd−CO and Pd_2−CO bonds. The most accurate density functionals for the systems tested in this paper are O3LYP, OLYP, PW6B95, and PBEh.

1. Introduction

Several of the most successful fuel cell applications use a Pt anode as a catalyst for the oxidation of hydrogen gas.[1−10] Unfortunately, there are several practical problems with using pure Pt anodes, so there has been considerable work in developing Pt alloys for use in fuel cells.[1,5−10] One important reason to use alloys is that they may be more resistant to CO poisoning than pure Pt. In this context, poisoning refers to the bonding of CO to active sites on the anode surface, which then block those sites for H_2 adsorption.[5,10] It is hoped that alloys will weaken the metal−CO bond without weakening the strength of H_2 adsorption. It is therefore important to be able to accurately calculate metal−CO bond energies. Because one of the alloys being considered for use in fuel cells is Pt/Pd,[5,7−9] we focus on the Pd_n−CO bond energy in this paper. In addition to its importance for fuel cells, metal−CO interactions are also more generally important interactions for catalysis.[11−14]

The present article is directed to determining suitable and efficient computational methods for Pd−CO bonds. We will examine the treatment of relativistic effects, the role of static correlation[15,16] (also called near-degeneracy correlation[17]), and the use of density functional theory (DFT), and many of the conclusions are also relevant to other 4d transition metals. To draw conclusions about suitable methods, we will first create a benchmark suite, based partly on experiment but mainly on wave function theory (WFT), especially coupled cluster theory,[15,18−20] with single and double excitations and a quasi-perturbative treatment of connected triple excitations, CCSD(T).

The PdCO molecule is the central molecule in our benchmark suite; it has been used as a model system many times in theoretical studies.[21−32] Computational studies are especially important for PdCO because there is no reported experimental bond energy for the dissociation of PdCO into Pd and CO. We denote this dissociation energy as D_e(Pd−CO). There are, however, experimentally determined bond lengths[33] for Pd−CO and PdC−O, denoted r_e(Pd−CO) and r_e(PdC−O), respectively. Despite the extensive theoretical scrutiny of PdCO, there is no consensus on the theoretical level required to predict or reproduce these values, and there is a large range of calculated values for D_e(Pd−CO) and r_e(Pd−CO), 27−55 kcal/mol and 1.78−1.91 Å, respectively.

One of the challenges that may account for the dispersion of these values is the large relativistic effect in Pd.[27] For example, Filatov[27] has demonstrated that relativity accounts for 36% of the calculated D_e(Pd−CO) at the CCSD(T) level of electronic structure theory. There are two ways that the relativistic effects can be treated, either by using a relativistic Hamiltonian as Filatov did or by using a relativistic effective core potential (RECP)[34] for scalar relativistic effects and adding spin−orbit coupling effects, when present, empirically or perturbatively.

Spin−orbit coupling vanishes (in first-order treatment) for Pd, CO, PdCO, Pd_2, and Pd_2CO as well as the first excited state of Pd_2, so we are primarily concerned with the scalar relativistic effect here. The use of a RECP is justified for treating scalar relativistic effects on metal−ligand bonding properties because the scalar relativistic effects mainly affect the core electrons, causing them to contract; the valence electrons are only indirectly effected by relativity because of the modification of their interaction with the core due to its contraction. This modified interaction causes the valence orbitals to also contract. From a computational standpoint, the RECP method is preferable to using a relativistic Hamilitonian because the calculations are much more tractable. In addition to the simpler form of the Hamiltonian, the reduced basis set size when core electrons are not represented explicitly makes a high-level treatment of the valence space more affordable. One of the issues that we will discuss in this article is how well the RECPs can capture the

* Author to whom correspondence should be addressed. E-mail: truhlar@umn.edu.

10.1021/jp064467t CCC: $33.50
Published on Web 11/03/2006

relativistic effect in PdCO. We note that some researchers[30,31,35] have used nonrelativistic effective core potentials (NRECPs) for PdCO, but those papers will not be discussed further, and use of NRECPs for systems involving Pd or any other 4d or 5d transition metal is discouraged.

There has been less study of the Pd_2CO system[22,29,36,37] than of PdCO, but a representative database of accurate metal−CO bond energies should contain systems with metal−metal bonds in addition to CO bonds to monatomic metals. A problem with bonds involving transition metal atoms is that the effects of static correlation (systems that exhibit significant static correlation are said to have multireference character) can significantly degrade the quality of metal−metal bond energies calculated with single-reference WFT and hybrid DFT methods,[38] although the effects of static correlation are sometimes less detrimental for metal−ligand systems.[39] ("Hybrid DFT" refers to DFT methods that contain a contribution from the nonlocal Hartree−Fock exchange funcional.[40]) Nava et al.[29] suggested that hybrid DFT methods are suitable only for systems involving a single Pd atom, but not for systems involving multiple Pd atoms, in particular Pd_2CO. This conclusion[29] will be reexamined in the present study.

We will first provide an outline of the previous work on the PdCO system to illustrate the need for justifying the RECP treatment for PdCO and then provide a brief discussion of previous work involving Pd_2 and Pd_2CO. The focus of the discussion on Pd_2 is not the relativistic effect but rather the ability to treat Pd_2 by single-reference methods. We will then calculate four types of quantities. (1) We will calculate bond energies, D_e, for PdCO, Pd_2, and Pd_2CO, where these quantities are denoted D_e(Pd−CO), D_e(Pd_2), and D_e(Pd_2−CO), respectively. In this notation the dash indicates which bond is being broken (in the case of D_e) in molecules with more than one bond. In all cases we consider the dissociation products, Pd and CO, or Pd_2 to be in their calculated ground electronic states. The subscript e denotes equilibrium values, i.e., zero-point-exclusive values. (2) We will also calculate the adiabatic excitation energies for the $4d^{10}5s^0 \rightarrow 4d^95s^1$ transition in the Pd atom and the $^3\Sigma_u^+ \rightarrow {}^1\Sigma_g^-$ transition in Pd_2, which are denoted $T_e(4d^{10}5s^0 \rightarrow 4d^95s^1)$ and $T_e(^3\Sigma_u^+ \rightarrow {}^1\Sigma_g^-)$, respectively. The focus of this paper is not on the excited-state properties for their own intrinsic interest but rather because they are relevant for the bonding in Pd_2 and Pd_2CO. (3) Third, we calculate bond lengths, r_e, for Pd−CO, PdC−O, Pd_2, Pd−PdCO, PdPd−CO, and Pd_2C−O, denoted r_e(Pd−CO), r_e(PdC−O), r_e(Pd_2), r_e(Pd−PdCO), and r_e(Pd_2C−O), respectively. See Figure 1 for bond length notation. (4) Finally, we calculate dipole moments, μ, for PdCO and Pd_2CO, where these quantities are dentoed μ(PdCO) and μ(Pd_2CO), respectively. These properties as computed by WFT will provide a robust data set test for testing both local and hybrid DFT methods. We will conclude with a discussion of whether various DFT methods can quantitatively describe bonding in PdCO and Pd_2CO.

2. Summary of Previous Results

2.A. The Pd Atom. We will begin with a brief discussion of the Pd atom. The Pd atom is not the focus of our paper but is germane for the subsequent discussions of Pd_2. The Pd atom ground state is $4d^{10}5s^0$.[41] The electronic state that corresponds to a bond between two $4d^{10}5s^0$ atoms is $^1\Sigma_g^+$, and the lowest-energy state corresponding to the interaction between two $4d^95s^1$ atoms is $^3\Sigma_u^+$. In Pd_2, the interaction between two $4d^{10}5s^0$ atoms would presumably form a weak bond,[42] whereas the interaction of two excited Pd atoms in the $4d^95s^1$ state would generate a stronger one.[42] It has been shown[43] that the $^3\Sigma_u^+$ electronic state is much lower than the $^1\Sigma_g^+$ state. Therfore the Pd_2 bond can only be accurately described if the $4d^{10}5d^0$ to $4d^95d^1$ transition is also accurate. The ground state of the Pd atom is not the same as the ground state of Ni, which has an electronic structure of $3d^84s^2$. As a consequence of the differing atomic configurations, Ni_2 and Pd_2 have different bond strengths and electronic structures.[42]

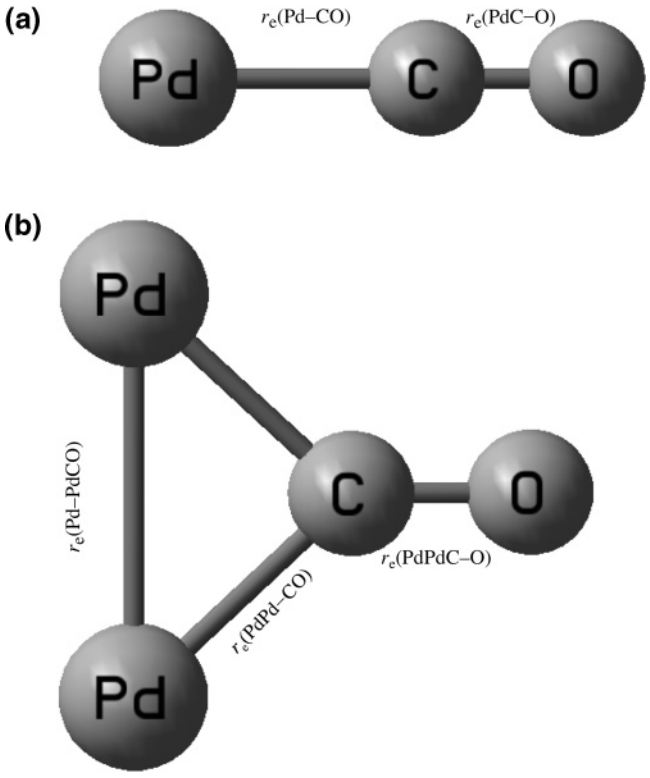

Figure 1. Geometries of (a) PdCO and (b) Pd_2CO.

Spin−orbit coupling does not vanish in the triplet D excited state of Pd. Therefore, to calculate $T_e(4d^{10}5s^0 \rightarrow 4d^95s^1)$ for Pd to compare with experiment,[41] we must add the contribution from spin−orbit coupling to our calculated value.[41] The ground state, $4d^{10}5s^0$, is a $^1S_0$ state and thus has no spin−orbit contribution; however, the first excited state, $4d^95s^1$, is a ^{3}D state and is thus a multiplet of nondegenerate terms with $J = 1$, 2, and 3, where J is the total angular momentum quantum number. The electronic structure calculations employed here do not include spin−orbit coupling, and the three energy levels in the multiplet are thus degenerate. We adjusted the calculated value for the ^{3}D state by assuming Russell−Saunders (LS) coupling and averaging over the experimental energies[41] of the J states of the ^{3}D multiplet. The assumption of LS coupling is valid when spin−orbit coupling is small, and it is therefore unclear whether LS coupling is valid for a metal like Pd because spin−orbit coupling is moderately large for 4d transition metals. However, the total effect of spin−orbit coupling on T_e, assuming LS coupling, is −3.15 kcal/mol, so the empirical LS treatment is probably valid. The spin−orbit value of −3.15 kcal/mol is added to the energy of the ^{3}D state before comparison to the experimental[41] $T_e(4d^{10}5s^0 \rightarrow 4d^95s^1)$ of 18.8 kcal/mol.

We will focus our discussion here on papers that will be significant for subsequent sections. We note initially that the scalar relativistic effect for $T_e(4d^{10}5s^0 \rightarrow 4d^95s^1)$ is nonnegligible.[22,44,45] Blomberg et al.[22] have calculated the scalar relativistic effect on $T_e(4d^{10}5s^0 \rightarrow 4d^95s^1)$ using the coupled pair functional[46] (CPF) method and a sufficiently large basis set and

TABLE 1: Summary of the Bond Energies, Denoted D_e(Pd−CO) and Given in kcal/mol, Reported in the Literature and the Corresponding Bond Lengths, Denoted r_e and Given in Å

first author	method	e$^-$ [a]	basis set[b]	T_e[c]	D_e(Pd−CO)	D_e(Pd−CO)/cp[d]	r_e(Pd−CO)	r_e(PdC−O)	D_e(Pd$_2$)	r_e(Pd$_2$)	D_e(Pd$_2$−CO)
Dai[36,43]	MRSDCI	lc	3s3p1d						19.8	2.48	71.9
McMichael[21]	MP2	lc	1s1p2d	16.7	37.4		1.882	1.185			
Blomberg[e22]	CPF	lc	11s8p4d	11.9	34		1.86				55
Blomberg[e22]	MCPF	lc	11s8p4d	11.9	34		1.86				
Blomberg[f22]	CPF	lc	11s8p4d3f	16.3	33	31	1.91				
Frankcombe[g24]	MP2	sc	4s4p3d				1.843				
Frankcombe[h24]	MP2	sc	5s4p4d3f				1.780				
Frankcombe[24]	CCSD(T)	sc	3s3p2d				1.883				
Filatov[27]	CCSD(T)	all	17s14p9d3f	18.1	42.0	38.5	1.838	1.143			
Cui[68]	CASPT2	sc	6s5p3d	17.1					22.6	2.43	
Cui[68]	B3LYP	sc	6s5p3d	15.7					20.6	2.52	
Chung[23]	*X*α	all	18s16p12d	13.7	68.3		1.81	1.15			
Chung[23]	BLYP	all	18s16p12d		48.4		1.86	1.16			
Efremenko[71]	B3LYP	sc	3s3p2d						19.1		
Nava[29,69]	B3LYP	sc	6s4p4d1f		42.0		1.854	1.114			59.5
Nava[29,69]	BP86	sc	6s4p4d1f		55.6		1.822	1.115	30.4	2.49	79.1
Rochefort[37]	BP86	sc	4s4p3d						34		75
Wu[28,72]	B3LYP	sc	4s4p3d		37.8		1.878	1.142	−4.10	2.38	
Wu[28,72]	B3P86	sc	4s4p3d		42.7		1.856	1.158	−4.80	2.35	
Wu[28,72]	B3PW91	sc	4s4p3d		40.6		1.859	1.143	6.48	2.36	
Wu[28,72]	BHLYP	sc	4s4p3d		27.2		1.909	1.125	29.77	2.34	
Wu[28,72]	BLYP	sc	4s4p3d		45.0		1.869	1.158	15.36	2.42	
Wu[28,72]	BP86	sc	4s4p3d		50.7		1.847	1.159	16.12	2.39	
Wu[28,72]	PBEh	sc	4s4p3d		41.0		1.858	1.141	−8.44	2.35	
Xiao[28,72]	BP86	all	7s6p4d	19.1					32.1	2.50	
experiment[32,41,60,64]				18.8			1.843 ± 0.003	1.138 ± 0.003	24 ± 4		

[a] e$^-$ refers to the number of electrons correlated, where lc = large core, sc = small core, and all = all of the electrons are correlated with no RECP. [b] This column gives the basis set used for Pd. All of the authors took a balanced basis set approach, so the C and O basis set is of comparable quality to the listed Pd basis set. [c] This quantity is denoted as $T_e(4d^{10}5s^0 \rightarrow 4d^95s^1)$ in the text. The computed values have been adjusted for spin−orbit effects by subtracting 3.15 kcal/mol from the published value. [d] Counterpoise-corrected results. [e] This is basis-A in the Blomberg et al. paper.[22] [f] This is basis-B in the Blomberg et al. paper.[22] [g] This is basis set 8 in the Frankcombe et al. paper[24] and was recommended for comparison to basis-A. [h] This is basis set 27 in the Frankcombe et al. paper.[24]

found that it decreases $T_e(4d^{10}5s^0 \rightarrow 4d^95s^1)$ by 17.8 kcal/mol. This decrease is nearly equivalent to the 16.8 kcal/mol scalar relativistic effect calculated by Filatov using the CCSD(T) level of electron correlation with a large basis set. (The relativistic effect is calculated as the difference between two calculations, where one of the calculations incorporates scalar relativistic terms into the Hamiltonian.) The relativistic $T_e(4d^{10}5s^0 \rightarrow 4d^95s^1)$ values computed by Blomberg and Filatov are 19.4 and 21.2 kcal/mol, respectively.

The scalar relativistic effect on $T_e(4d^{10}5s^0 \rightarrow 4d^95s^1)$ computed by Xiao et al.[45] using the Becke−Perdew 1986 (BP86)[47,48] density functional and by Chung et al.[23] using a local spin density approximation (LSDA) density functional are 15.9 and 15.5 kcal/mol, respectively. The scalar relativistic $T_e(4d^{10}5s^0 \rightarrow 4d^95s^1)$ values computed by Xiao et al.[45] and Chung et al.[23] are 22.8 and 16.8 kcal/mol, respectively. We can see from these three results that the relativistic effect for $T_e(4d^{10}5s^0 \rightarrow 4d^95s^1)$ is 15−18 kcal/mol depending on which method is used, and the calculated $T_e(4d^{10}5s^0 \rightarrow 4d^95s^1)$ is typically in the range of 16−23 kcal/mol. These results show that the relativistic effect on $T_e(4d^{10}5s^0 \rightarrow 4d^95s^1)$ is nearly as large as the value itself.

An additional topic that will be discussed in this paper is how accurately Pd systems can be treated by single-reference methods, such as CCSD(T). For both Pd and PdCO, Blomberg et al.[22] reported both CPF and modified CPF[17] calculations, which gave "nearly identical" results. The CPF and MCPF methods, like CCSD(T), are based on a single-configuration reference wave function, but the MCPF method has been shown to yield excellent agreement with multireference configuration interaction (MRCI) calculations.[17] Table 1 shows that the CPF calculation of Blomberg et al.[22] differs from CCSD(T) by less than 2 kcal/mol, which indicates that the Pd atom can be treated to a good approximation by single-reference methods. Further evidence is that the CCSD(T) calculation is within 1 kcal/mol of the experimental value. This result is significant because the Ni atom in the same column of the periodic table has significant multireference character, and the adiabatic excitation energy cannot be treated using single-reference methods.[49]

2.B. PdCO. One of the first and most influential papers on PdCO was by Blomberg et al.,[22] in which PdCO was treated using the CPF method with a relativistic Hamilitonian. The computed scalar relativistic effects were an 11 kcal/mol increase in D_e(Pd−CO) and an 0.09 Å contraction in r_e(Pd−CO). Blomberg et al.[22] also pointed out that, unlike NiCO, PdCO has very little multireference character. This means that single-reference treatments such as CPF, closed-shell second-order perturbation theory[50,51] (MP2), and CCSD(T) should be sufficient.

Blomberg et al.[22] also illustrated the sensitivity of the r_e(Pd−CO) to basis set size. In their paper, two basis sets were used, basis-A and basis-B, where basis-A was of size 11s8p4d and basis-B was of size 11s8p4d3f. The difference in bond energies was 1 kcal/mol (D_e(Pd−CO) = 34 kcal/mol with basis-A and D_e(Pd−CO) = 33 kcal/mol with basis-B), and the difference in r_e(Pd−CO) was 0.05 Å (1.86 Å with basis-A and 1.91 Å with basis-B).

The more recent paper by Filatov[27] reported results obtained using the CCSD(T) method with a relativistic Hamilitonian. We compare the results of Filatov to the larger basis set result of Blomberg et al. because Filatov included f functions in his basis set. The difference in r_e(Pd−CO) is surprisingly large, 1.84 Å for Filatov and 1.91 Å for Blomberg et al. The D_e(Pd−CO) values also show large differences between the calculations by the two groups; in particular, they disagree by 7 or 9 kcal/mol depending on whether counterpoise corrections are included. There are several possible scenarios as to why there is a

discrepancy: (1) Blomberg and Filatov use different methods of computing the scalar relativistic effects; Blomberg et al. used first-order perturbation theory,[52,53] and Filatov used the IORAmmm[52,54] one-electron Hamiltonian. (2) Blomberg et al. may not have correlated enough electrons in their study, as they only correlated the 4d,[10] $2s^22p^2$, and $2s^22p^4$ electrons on Pd, C, and O, respectively, whereas Filatov correlated all of the electrons. (3) Although the basis sets are seemingly large enough for quantitative work, at least one of them is not complete enough to calculate an accurate bond distance. (4) One may question whether PdCO can be treated by single-reference methods as originally suggested. We will report new calculations designed to address issues 2−4 in this paper. The first issue is not expected to be a problem because there was reasonable agreement between Blomberg et al. and Filatov with respect to the relativistic corrections; in particular the relativistic increases in D_e(PdCO) computed by Blomberg et al. and Filatov were 11 and 14 kcal/mol, respectively. In addition, the relativistic contraction in r_e(Pd−CO) was 0.07 Å in both cases. There is also good agreement between Blomberg et al. and Filatov with respect to the relativistic corrections to $T_e(4d^{10}5d^0 \rightarrow 4d^95s^1)$.

We are also interested in determining how well the RECP treatment can be applied to PdCO systems. In general, the scalar relativistic effects in PdCO are quite different from those of Pd or Pd_2. For Pd and Pd_2 the primary relativistic effect is the lowering of the 5s orbital energy. This effect is explicity accounted for in the parametrization of the RECP by including $T_e(4d^{10}5d^0 \rightarrow 4d^95s^1)$ in the fitting data.[55] However, the Pd−CO bond in PdCO is considered to be a charge-transfer bond, and it is not clear based on previous work how well RECPs can describe this situation.

The first RECP treatment of PdCO was carried out by McMichael et al.[21] using a large-core RECP[56] and the MP2 level of electron correlation. It is difficult to use this study to validate the RECP treatment because the basis set used by McMichael et al.[21] is much smaller than any basis set used by Filatov or Blomberg. Perhaps, the most direct comparison would be to Blomberg's result with basis-A, because the degree of polarization in the bases and the numbers of correlated electrons are similar. The values of r_e(Pd−CO) and D_e(Pd−CO) calculated by McMichael with the RECP were 1.882 Å and 37.4 kcal/mol, respectively, and they overestimated the Blomberg et al. basis-A results[22] (r_e(Pd−CO) = 1.86 Å and D_e = 34 kcal/mol) by 0.02 Å and 3 kcal/mol, respectively. If we compare the McMichael results to those of either Filatov or Blomberg et al.[22] with basis-B, then the differences in both quantities, D_e(Pd−CO) and r_e(Pd−CO), are less than the expected relativistic corrections. It would seem that results of McMichael et al.[21] justify the RECP approach, but the results are suspect because the valence electron basis set used by McMichael et al. was so small. It would not be unreasonable to expect a substantional basis set superposition error in the McMichael et al. calculation. It would also seem likely that increasing the basis set size would worsen the agreement between the results of McMichael et al. and the NRECP calculations.

Additional work was done by on PdCO by Frankcombe et al.[24] using the MP2 level of theory and a small-core RECP.[57] They recommended comparing the results with their "basis set 8" to Blomberg's results with basis-A because the valence basis functions used in both bases were similar. The reported value for r_e(Pd−CO) by Frankcombe et al.[24] using basis set 8 was 1.84 Å, which underestimated the result of Blomberg et al.[22] using basis-A by 0.02 Å. This, coupled with the results of McMichael et al., may seem like a reasonable justification of the RECP approach for PdCO. But, Frankcombe et al. also reported the Pd−CO bond length with a much larger basis set, called basis set 27 in their paper, as 1.780 Å, which disagrees with the result of Blomberg et al.[22] using basis-B by −0.13 Å and Filatov's result by −0.06 Å. It is difficult to trust the MP2 results with a RECP because r_e(Pd−CO) is significantly contracted when the basis set is increased, whereas increasing the basis set with the CPF method and explicit relativistic effects increases r_e(Pd−CO). Frankcombe et al.[24] also calculated r_e(Pd−CO) using the CCSD(T) correlation method and a modest basis set. Their CCSD(T) bond length disagreed with the basis-A and basis-B results of Blomberg et al.[22] by 0.02 and −0.03 Å, respectively, and with Filatov's result by 0.04 Å. Frankcombe et al.[24] were interested in the reaction energy of $PdPH_3 + CO \rightarrow PH_3 + PdCO$, so no Pd−CO bond energy was reported. For us to trust the RECP treatment of PdCO with WFT methods, we would have to rely either on questionable MP2 results or entirely on the r_e(Pd−CO) value computed with CCSD(T) and a modest basis set.

In addition to discussing WFT results, we will analyze how accurately the PdCO bond can understood using DFT. Chung et al.[23] used DFT to explore the relativistic effect in PdCO. Using the $X\alpha$[58] functional (which is an empirically modified LSDA functional), they found that the relativistic increase in D_e(Pd−CO) was 15 kcal/mol and the contraction in r_e(Pd−CO) was 0.06 Å. These effects are similar to the relativistic effects calculated by Filatov[27] using CCSD(T) and by Blomberg et al.[22] using CPF. Chung et al.[23] reported a relativistic D_e(Pd−CO) of 48.4 kcal/mol using the Becke−Lee−Yang−Parr (BLYP)[47,59] functional, which agrees well with the D_e(Pd−CO) value of 45.0 kcal/mol computed by Wu et al.[28] using the BLYP method and a RECP. The r_e(Pd−CO) values computed by Chung et al. and Wu et al.[28] are also in good agreement with one another, 1.87 and 1.86 Å, respectively. One might expect the results to agree better than 3 kcal/mol for the bond energies, but there are nuances to each of the calculations that may account for the differences. The most notable difference is that Chung et al. calculated the properties with the BLYP exchange−correlation functional, but the electron density was optimized with the $X\alpha$ functional, whereas Wu et al. optimized the density with the BLYP exchange−correlation functional.

We will be able to draw more definitive conclusions by designing calculations specifically to address the issues under consideration.

2.C. Pd_2. There have been several previous studies of the Pd dimer. The earliest reported bond energy of Pd_2 was an experimental measurement by Kant et al.,[60] where they reported a 0 K bond energy of 17 ± 6 kcal/mol. An experimental value for the 0 K bond energy, 24 ± 4 kcal/mol, was also reported by Shim et al.[61] Kant et al.[60] assumed a $^1\Sigma$ electronic state for Pd_2, and Shim et al.[61] determined a $^1\Sigma$ electronic ground state for Pd_2 from a nonrelativistic Hartree−Fock calculation. After critical reviews,[42,62] the recommended value is 24 ± 4 kcal/mol. The ground electronic state of Pd_2, however, has been determined through experiment[63,64] and calculations[43,64] to be a $^3\Sigma_u^+$ state. We list the experimental bond energies in Table 1; however, they have been adjusted for zero-point effects using the harmonic frequency reported by Ho et al.[63] for the $^3\Sigma_u^+$ state.

We will only discuss the most relevant of the many theoretical studies of Pd_2. The papers that we discuss here are summarized in Table 1. The first paper, by Xiao et al.,[45] is on the relativistic effect in Pd_2. The properties of Pd_2 were calculated with the BP86 local functional and an all-electron basis set. Xiao et al.

have shown that the electronic ground state of Pd_2 is $^3\Sigma_u^+$ when relativistic effects are included and the electronic ground state is $^1\Sigma_g^+$ when relativistic effects are not included. Their finding of a $^3\Sigma_u^+$ ground state using relativistic methods is in agreement with other DFT calculations using RECPs.[65−71] The relativistic effect in the ground-state value of $D_e(Pd_2)$ values is 21 kcal/mol.

The issue of relativistic effects explains,[45] to some extent, the initial determination of a singlet ground electronic state by Shim et al.[61] As mentioned in sections 2.A and 2.B, the ground state of the Pd atom is $(4d^{10}5s^0)$,[41] and the interaction of two ground-state Pd atoms might be expected to generate a weak van der Waals interaction;[42] however, the interaction between two Pd atoms in their first excited state, $4d^95s^1$,[41] will produce a much stronger σ-type bond.[42] Because the atomic promotion energy is strongly affected by relativistic effects,[44] the relativistic stabilization of the 5s orbitals in the Pd atom leads to a relativistic stabilization of the 5s-derived σ-orbitals in Pd_2. Thus, the ground electronic state is determined largely by the $4d^{10}5s^0 \rightarrow 4d^95s^1$ promotion energy.

Table 1 shows DFT results that are computed with the BP86 functional. The calculations by Nava et al.[69] and Wu[72] are with RECPs, and the other calculation, by Xiao et al.,[45] employs an all-electron basis set with a relativistic Hamilitonian. Comparing these Pd_2 calculations, we can see that the bond energies and bond lengths computed by Nava et al.[69] and Xiao et al.[45] agree with each other to within 2 kcal/mol for $D_e(Pd_2)$ and 0.01 Å, respectively. The bond energy computed by Wu[72] is significantly lower (∼15 kcal/mol) than the other two values, and the bond length reported by Wu[72] is ∼0.10 Å lower than the other two values. The major difference between the Wu[72] study and Nava et al.[69] is the choice of RECP. Wu[72] uses the RECP by Stevens−Basch−Krauss−Jasien−Cundari,[73−75] and Nava et al.[69] use one of the Stuttgart RECPs.[76] (See section 3.D for more detail.) The results of Wu[72] are also inconsistent with the other DFT studies in Table 1; hence they will not be considered further.

Two multireference WFT calculations are relevant.[36,68] The first calculation, by Balasubramanian,[43] is a multireference singles plus doubles configuration interaction calculation with a Davidson correction[77,78] (MRSDCI+Q). The second calculation is complete activation space second-order perturbation theory[79] (CASPT2) calculation by Cui et al.[68] In both of these calculations, $D_e(Pd_2)$ is approximately 20 kcal/mol. This is significant because the B3LYP calculations in Table 1 predict $D_e(Pd_2)$ to be approximately 20 kcal/mol, whereas the local methods in Table 1 predict $D_e(Pd_2)$ to be near 30 kcal/mol. Local functionals often predict bond lengths that are too large, but it has also been found[38,70,80,81] that local methods are often preferred for bonds involving transition metal atoms because the effects of static correlation significantly reduce the quality of the hybrid DFT calculation. In previous work,[38] it was shown that the effects of static correlation are not uniform for all transition metal atoms, and Pd_2 would seem to be a case where hybrid DFT outperforms local DFT. This is not expected because Ni_2, where Ni is directly above Pd in the periodic table, has strong multireference character.[38] The assignment of Pd_2 as single-reference system is still tentative (and therefore will be readdressed with new calculations below) because the basis sets and number of electrons correlated in the previous studies[43,68] may be too small for quantitative work.

2.D. Pd_2CO. Of the three molecules studied in this paper, the Pd_2CO system has received the least attention.[22,29,36,37] The previous calculations are summarized in Table 1, and we will discuss the results of Blomberg et al.[22] first; they computed $D_e(Pd_2-CO)$ with the CPF method and basis-A. We have included the Blomberg et al. value[22] for the sake of completeness, but they assumed a $^1\Sigma_g^+$ ground electronic state for the Pd_2 dissociation product, whereas the correct electronic ground state is $^3\Sigma_u^+$. They also used a geometry that was obtained in a previous calculation[31] where NRECPs were used instead of RECPs. Dai et al.[36] have also calculated $D_e(Pd_2-CO)$ using the MRSDCI+Q method of electronic correlation and a RECP. The value for $D_e(Pd_2-CO)$ computed by Dai et al.[36] is 75.5 kcal/mol, which is 20 kcal/mol larger than the $D_e(Pd_2-CO)$ of 55 kcal/mol computed by Blomberg et al.[22] The reported value by Dai et al.[36] is also for dissociation into the singlet state of Pd_2 and not the ground electronic state. We have adjusted the $D_e(Pd_2-CO)$ of Dai et al.[36] for dissociation into the ground electronic state of Pd_2 using earlier results[43] from one of the authors. In doing so, we obtain a $D_e(Pd_2-CO)$ of 71.9 kcal/mol. The difference of 20 kcal/mol between the CPF value of $D_e(Pd_2-CO)$ and the MRSDCI+Q value of $D_e(Pd_2-CO)$ is larger than expected and warrants a reinvestigation of this value using ab initio WFT.

The remaining papers[29,37,82] that we will discuss are DFT studies in which hybrid and local DFT functionals were used. In the paper by Nava et al.[29] the issue was raised that hybrid methods such as B3LYP will perform poorly for Pd_2CO due the inadequacy of Hartree−Fock wave functions to accurately describe the bonding between transition metal atoms. As discussed in section 2.C, there are several issues involved when applying hybrid DFT methods to systems involving multiple metal−metal bonds. These issues arise again in considering Pd_2CO because the B3LYP bond energy disagrees with the MRSDCI+Q bond energy[36] by 13 kcal/mol, whereas the BP86 functional disagrees with the MRSDCI+Q bond energy[36] by 9 kcal/mol. The best agreement between previous DFT calculations and the MRSDCI+Q bond energy[36] of 72 kcal/mol is the $D_e(Pd_2-CO)$ value of 75 kcal/mol computed by Rochefort[37] with the Perdew−Burke−Enzerhof[83] (PBE) local functional. However, this result is somewhat inconsistent with the results of Cui et al.[68] One might expect that if Pd_2CO had significant amounts of static correlation that Pd_2 would also have significant amounts of static correlation, but the results of Cui et al.[68] indicate that Pd_2 does not have significant amounts of static correlation. We will also present new calculations designed to address whether the Pd_2CO system has significant multireference character, in addition to the calculations on the Pd_2 and PdCO molecules.

3. Computational Methods

3.A. Electron Correlation and Density Functional Theory Methods. In this paper, the only WFT-based methods that we use are CCSD(T) and CASPT2 (the latter results are discussed only in the Appendix, which is in the Supporting Information). The number of density functionals that we is use quite large due to the number of exchange and correlation functionals that are available in the literature that are deemed to be viable candidates for studying fuel cells. In section 4 we test a selection of popular DFT methods: the BLYP series, BLYP, [47,59] B3LYP,[47,59,84] B1LYP,[47,59,85] and B3LYP*;[47,59,86] the BP86 series, BP86[47,48] and B3P86; [47,48,84] the mWPW series, mPWPW,[87,88] mPW1PW,[87,88] and MPW1K;[87−89] the OLYP series, OLYP[59,90] and O3LYP; [59,90,91] the PBE series, PBE[83] and PBEh;[83,92] the TPSS series, TPSS[93] and TPSSh;[93] Minnesota functionals, M05,[94] M05-2X,[94] PW6B95,[95] and PWB6K;[95] Becke−Handy−Tozer−Martin-type functionals, B98,[96]

TABLE 2: T_1-Diagnostics, B_1-Diagnostics, and CCSD(T) Equilibrium Dissociation Energies and Excitation Energies for the Molecules in AE6 and Several Transition-Metal-Containing Molecules

molecule	basis set	T_1-diagnostic	B_1-diagnostic[e]	HF orbitals	KS orbitals
		Atomization Energies			
propyne (C_3H_4)	aug-cc-pVTZ	0.011	1.7	617.6	617.8
glyoxal ($C_2H_2O_2$)	aug-cc-pVTZ	0.016	5.0	689.3	689.2
cyclobutane (C_4H_8)	aug-cc-pVTZ	0.008	0.6	1128.6	1128.5
silane (SiH_4)	aug-cc-pVTZ	0.011	0.6	318.1	317.6
SiO	aug-cc-pVTZ	0.026	13.8	182.8	183.0
S_2	aug-cc-pVTZ	0.008	8.2	94.4	94.2
V_2	cc-pwCVTZ	0.040	64.6	49.4[a]	59.0[b]
Cu_2	cc-pwCVTZ	0.021	7.7	41.7[c]	43.5[d]
		Transition Energies			
Pd ($4d^{10}5s^0$)	MQZ-h	0.009			
Pd ($4d^95s^1$)	MQZ-h	0.017		16.1	16.6
		Bond Energies			
PdCO[f]	MQZ-h	0.023	10.2	44.8[i]	45.8[i]
Pd_2[g]	MQZ-h	0.054	9.3	18.6[i]	19.6[i]
Pd_2CO[h]	MQZ-h	0.026	10.7	71.0[i]	71.9[i]

[a] The optimum geometry is 1.752 Å. [b] The optimum geometry is 1.753 Å. [c] The optimum geometry is 2.529 Å. [d] The optimum geometry is 2.526 Å. [e] Divided by the number of bonds broken and 1 kcal/mol. The process is atomization except for PdCO, where it involves dissociation to Pd + CO, and Pd_2CO, where it involves dissociation to Pd_2 + CO. The latter two processes each break one bond, as does atomization of SiO, S_2, V_2, and Cu_2. [f] Dissociation into Pd($4d^{10}5s^0$) + CO. [g] Dissociation into Pd($4d^{10}5s^0$) atoms. [h] Dissociation into $Pd_2(^3\Sigma_u^+)$ + CO. [i] CCSD(T)/MQZ-sc-optimized geometries.

B97-1,[97] B97-2,[98] and BMK;[99] the Xu−Goddard functional, XLYP;[59,100] and a few encouragingly accurate functionals from our recent paper[101] on organometallic and inorganometallic chemistry, G96LYP,[59,102] MOHLYP,[59,90,101] and MPWLYP1M.[59,87,101] In the mPW and PBE series, the functionals differ only in the percentage X of Hartree−Fock exchange. Note that some functionals have more than one name in the literature; thus mPWPW is also called mPWPW91, mPW1PW is also called MPW1PW91, mPW0, and MPW25, and PBEh is also called PBE0 and PBE1PBE.

3.B. Software. The CCSD(T) and CASPT2 calculations were carried out with Molpro, version 2002.6.[103] The DFT calculations were carried out with and a locally modified version of Gaussian 03, revision C.01,[104] respectively, except for the XLYP calculations. The XLYP calculations were carried out with NWChem, version 4.7.[105]

3.C. Dipole Moments. The dipole moments for the DFT calculations are computed as expectation values from the wave function. For the CCSD(T) calculations, the dipole moments are calculated by applying the finite field technique and using electric fields of 0, ±0.0025, and ±0.005 au. We report the dipole moments to three significant figures as the calculations with electric fields of ±0.0025 and ±0.005 au agreed to within 0.01 D.

3.D. Basis Sets and Effective Core Potentials. We will discuss several basis set/RECP combinations in this paper. One basis set/RECP combination is the TZQ[101] basis set, which uses a (8s8p6d4f/4s4p4d3f) valence electron basis set for Pd and the MG3 basis set[106] for C and O. (The MG3 basis set is equivalent to the 6-311+G(2df) basis[107] set for C and O.) The RECP used for Pd in the TZQ basis set is the one developed by Stevens−Basch−Krauss−Jasien−Cundari.[73−75] This RECP is referred to in some publications as SBKJC and as CEP in others, where CEP stands for compact effective potential. We also use two basis sets from the recent paper by Quintal et al.[108] that are denoted as MTZ and MQZ. The MTZ basis set uses a (9s8p7d3f2g/7s6p4d3f2g) valence electron basis set for Pd and the aug-cc-pVTZ basis set[109] for C and O. The MQZ basis set uses a (12s11p9d5f4g3h/8s7p7d5f4g3h) valence electron basis set for Pd and the aug-cc-pVQZ[109] basis set for C and O. The RECP used in the MTZ and MQZ basis sets is the $M^{(Z-28)}$−Wood−Boring model,[55] denoted MWB28. We note that the MWB28 RECP is part of the Stuttgart−Dresden−Dunning (SDD) family[76] of RECPs.

We will also use different basis sets for discussing the issue of multireference character in these systems. For Pd, we will use a modified form of the MQZ basis set called MQZh, which is the MQZ basis set with no h-functions. The aug-cc-pVQZ basis set for C and O is used with the MQZh basis set. We will also compute the bond energies of V_2 and Cu_2 with the all-electron cc-pwCVTZ basis sets of Balabanov and Peterson.[110]

3.E. Core Electrons. The RECPs used in this paper are termed small-core RECPs, which this means that the [Ar]$3d^{10}$ electrons are replaced with the RECP and the $4s^24p^6$ electrons are not included in the RECP. (A large-core RECP would include the $4s^24p^6$ electrons in the RECP.) The $4s^24p^6$ electrons are always treated explicitly in the self-consistent field step of the DFT and CCSD(T) calculations in this article, but we will explore two choices for the issue of correlating these electrons using CCSD(T). The notation that we will adopt is CCSD(T)/basis-sc if the $4s^24p^6$ electrons are correlated and CCSD(T)/basis-lc if the $4s^24p^6$ electrons are not correlated, where "basis" can be TZQ, MTZ, or MQZ. In this context, "sc" and "lc" refer to small core and large core. We always use a small-core RECP, but the "sc" and "lc" notation indicates how many electrons are correlated in the post-self-consistent field steps.

4. Results and Discussion

4.A. Static Correlation. A topic that was mentioned several times in section 2 is the effect of static correlation on the computed bond energies. In this section, we compare three different diagnostics for determining whether a system has significant multireference character, and in addition to Pd, PdCO, Pd_2, and Pd_2CO, we also include the six molecules of the AE6 database and two transition metal dimers (V_2 and Cu_2) in the comparison. The AE6 database was chosen, because it is a collection of main group atomization energies, and all of the molecules are considered single-reference cases. The V_2 and Cu_2 molecules were included because in previous work[38] V_2 was determined to be a severely multireference dimer while Cu_2 was determined to be a single-reference dimer.

In Table 2, we give the T_1-diagnostic[111] and the B_1-diagnostic[101] values for the molecules in AE6, V_2, Cu_2, and the

Pd systems that we have studied in this paper. The recommended values of the T_1-diagnostic and B_1-diagnostic are 0.02 and 10.0, (the B_1-diagnostic value is divided by 1 kcal/mol to produce a unitless diagnostic); that is, a system or bond dissociation process should be considered to require multireference methods (in WFT) or no Hartree−Fock exchange (in DFT) if the diagnostic exceeds these values.[101,111] (Note that the T_1-diagnostic value refers to the system itself, whereas the B_1-diagnostic value refers to a bond-breaking process, either breaking one bond or atomization, which breaks them all. The B_1-diagnostic value is always divided by the number of bonds broken to express it on per bond basis.)

For five of the six molecules in AE6, the T_1-diagnostic values are less than 0.02. For SiO, the T_1-diagnostic value is 0.026. Furthermore, SiO has a B_1-diagnostic value of 13.8, and SiO is the only molecule in the AE6 database that has a B_1-diagnostic value greater than 10. (Thus SiO has mild multireference character.)

We can see that the T_1- and B_1-diagnostics both make a clear distinction between V_2 and Cu_2. For V_2, the T_1- and B_1-diagnostic values are 0.040 and 64.6, respectively, which are much larger than the nonminal single-reference/multireference borderline values of 0.02 and 10.0. For Cu_2, the T_1- and B_1-diagnostic values are 0.021 and 7.7 kcal/mol, which are near the border. These two diagnostics indicate that V_2 is a severe multireference case and Cu_2 is a single-reference case, which agrees with our previous assessment[38] and confirms the usefulness of both diagnostics.

With these diagnostics at our disposal, the PdCO and Pd_2-CO systems appear to be single-reference or borderline cases. The T_1-diagnostic values for PdCO and Pd_2CO are 0.023 and 0.026, respectively, and the corresponding B_1-diagnostic values are 10.2 and 10.7, respectively. Pd_2 is a single-reference system based on the B_1-diagnostic value of 9.3, but it should be treated with multireference methods based on the T_1-diagnostic value of 0.054. There is also some question regarding the recommended T_1-diagnostic value for open-shell systems, and the T_1-diagnostic may not be a reliable indicator of multireference character for these systems.[112]

As an alternative diagnostic, we compute and compare the properties from CCSD(T) using two different sets of reference orbitals. Our supposition is that single-reference systems will be insensitive to the choice of reference orbitals and the multireference systems will be sensitive to the choice of reference orbitals. For our tests, one set of orbitals is obtained from a Hartree−Fock calculation, and the other is obtained from a DFT calculation. This approach has been described by Villaume et al.[113] and utilized by Beran et al.[114] As an initial validation of the this technique, we compute the atomization energies for the molecules in AE6 using Hartree−Fock and Kohn−Sham orbitals, where the Kohn−Sham orbitals are obtained from a BLYP calculation. The AE6 atomization energies computed with Hartree−Fock orbitals and Kohn−Sham orbitals are given in the last two columns of Table 2. We note that there is good agreement between both sets of calculations. The largest difference for atomization energies is for silane, where the CCSD(T) calculations based on the two sets of orbitals yield atomization energies of 318.1 and 317.5 kcal/mol. This is a difference of 0.6 kcal/mol, and we find a 0.1−0.2 kcal/mol difference in atomization energies between the Hartree−Fock and Kohn−Sham reference calculations for the remaining five molecules in AE6.

For the two transition metal dimers, V_2 and Cu_2, we can see V_2 is much more sensitive to the choice of reference orbitals than Cu_2 or any of the molecules in AE6. The V_2 atomization energies with the Hartree−Fock and Kohn−Sham references are 49.4 and 59.0 kcal/mol, respectively. (The accurate experimental bond energy for V_2 is 64.2 kcal/mol.[64]) This difference of 9.6 kcal/mol is significantly larger than what we see with AE6 and Cu_2. For Cu_2, the atomization energies calculated with the Hartree−Fock and Kohn−Sham references are 41.7 and 43.5 kcal/mol, which is a difference of 1.7 kcal/mol. (The accurate experimental bond energy for Cu_2 is 47.2 kcal/mol.[64]) The value of 1.8 kcal/mol is still larger than that for any molecule in AE6, but 1.8 versus 9.6 kcal/mol demonstrates that Cu_2 has less multireference character than V_2.

The CCSD(T) geometries for V_2 and Cu_2 were also optimized using Hartree−Fock and Kohn−Sham orbitals before computing their respective atomization energies. We found that the geometries do not depend sensitively on the choice of reference orbitals. For V_2, the CCSD(T) bond lengths with the Hartree−Fock and Kohn−Sham orbitals are 1.752 and 1.753 Å, respectively. For Cu_2, the bond lengths with the Hartree−Fock and Kohn−Sham orbitals are 2.229 and 2.226 Å, respectively. The experimental bond lengths for V_2 and Cu_2 are 1.77 and 2.22 Å, respectively.[64]

For the four Pd systems, we have computed $T_e(4d^{10}5s^0 \rightarrow 4d^95s^1)$, $D_e(Pd-CO)$, $D_e(Pd_2)$, and $D_e(Pd_2-CO)$ using the MQZh basis set. On the basis of our experience with V_2 and Cu_2, we did not expect the geometries to be very sensitive to the choice of reference orbitals; therefore, we used the CCSD(T)/MQZh-sc geometries for these calculations. From Table 2, we can see that the Pd systems are less sensitive to the reference orbitals than the Cu_2 and V_2 systems. The PdCO and Pd_2 bond energies are the most sensitive to the choice of reference orbitals. The difference in bond energies between the Hartree−Fock and Kohn−Sham reference calculations is 1.0 kcal/mol for both of these systems, which is similar in magnitude to the largest difference in AE6.

The results in this section may be summarized as follows: The T_1-diagnostic predicts large multireference character for Pd_2 and borderline character for PdCO and Pd_2CO, the B_1-diagnostic indicates that all of these systems are borderline, and the reference-orbital diagnostic indicates that all three are single-reference types. The T_1-diagnostic and reference-orbital diagnostic indicate that the Pd atom has single-reference character. We accept the reference-orbital tests as the most reliable, and we conclude that all four systems may be treated reliably by single-reference methods such as CCSD(T).

4.B. CCSD(T) Results. The CCSD(T) results with six combinations of which electrons are correlated and which basis sets are used are given in Table 3.

4.B.1. Pd Atom. We will first discuss the atomic excitation energies, $T_e(4d^{10}5s^0 \rightarrow 4d^95s^1)$. We note first that the effect of correlating the $4s^24p^6$ electrons on Pd is nonneglible and lowers $T_e(4d^{10}5s^0 \rightarrow 4d^95s^1)$ by 4−6 kcal/mol depending on which basis set is used. $T_e(4d^{10}5s^0 \rightarrow 4d^95s^1)$ depends slightly on the basis set, as the values computed with CCSD(T)/TZQ-lc, CCSD(T)/MTZ-lc, and CCSD(T)/MQZ-lc are 24.6, 20.4, and 21.9 kcal/mol, respectively. The overall basis set dependence for the large-core calculations is ∼2 kcal/mol. The basis set dependence for the small-core calculations is also ∼2 kcal/mol, as the computed transition energies with CCSD(T)/TZQ-sc, CCSD(T)/MTZ-sc, and CCSD(T)/MQZ-sc are 17.0, 16.2, and 17.8 kcal/mol, respectively.

The most accurate value, $T_e(4d^{10}5s^0 \rightarrow 4d^95s^1) = 17.8$ kcal/mol, is obtained with the MQZ basis set and correlation of the $4s^24p^6$ electrons as well as the $4d^{10}5s^0$ electrons. The error in

TABLE 3: CCSD(T) Results, the Bond Dissociation Energy, D_e, for the Dissociation of PdCO into Pd and CO, Given in kcal/mol, and the Bond Lengths, r_e, for PdCO, Given in Å

	PdCO					
	r_e(Pd−CO)	r_e(PdC−O)	D_e(Pd−CO)	D_e(Pd−CO)/cp[a]	μ	Δr_e(CO)[b]
			Large Core[c]			
TZQ	1.862	1.145	39.7	34.2	2.48	0.011
MTZ	1.839	1.148	42.6	41.0	2.53	0.012
MQZ	1.840	1.144	41.0	40.3	2.49	0.012
			Small Core[d]			
TZQ	1.841	1.146	50.0	37.0	2.57	0.012
MTZ	1.799	1.133	53.0	40.7	2.55	0.013
MQZ	1.834	1.144	43.8	42.8	2.50	0.012

	Pd_2		
	$r_e(Pd_2)$	$D_e(Pd_2)$	$D_e(Pd_2)$/cp[a]
		Large Core[c]	
TZQ	2.456	10.2	4.3
MTZ	2.438	13.9	10.9
MQZ	2.417	11.3	10.9
		Small Core[d]	
TZQ	2.441	26.4	11.7
MTZ	2.419	27.1	17.0
MQZ	2.417	17.5	16.9

	Pd_2CO						
	r_e(Pd−PdCO)	$r_e(Pd_2-CO)$	$r_e(Pd_2C-O)$	$D_e(Pd_2-CO)$	$D_e(Pd_2-CO)$/cp[a]	μ	Δr_e(CO)[a]
				Large Core[c]			
TZQ	2.629	1.934	1.169	69.3	62.4	2.81	0.035
MTZ	2.588	1.912	1.173	72.7	65.5	2.86	0.037
MQZ	2.582	1.913	1.168	71.2	69.8	2.84	0.036
				Small Core[d]			
TZQ				73.4	59.4	2.78	
MTZ				82.5	63.0	2.82	
MQZ				70.3	68.5	2.81	

Pd			
$T_e(4d^{10}5s^0 \rightarrow 4d^9 5s^1)$[e]		$T_e(4d^{10}5s^0 \rightarrow 4d^9 5s^1)$[e]	
Large Core[c]		Small Core[d]	
TZQ	24.60	TZQ	17.02
MTZ	20.44	MTZ	16.25
MQZ	21.90	MQZ	17.79

[a] Counterpoise-corrected results. [b] $\Delta r_e(CO) = r_e(Pd_nC-O) - r_e(CO)$, where $n = 1$ or 2 and $r_e(CO)$ is the equilibrium bond length of CO. [c] The $4s^24p^6$ electrons on Pd and the $1s^2$ electrons on C and O were not correlated. [d] The $1s^2$ electrons on C and O were frozen during the correlation treatment. [e] A quantity of 3.15 kcal/mol was subtracted from the calculated value to account for spin−orbit coupling.

CCSD(T)/MQZ-sc is less than 1 kcal/mol when compared to the experimental value. The CCSD(T)/MQZ-sc result is also in good agreement with Filatov's value[27] for $T_e(4d^{10}5s^0 \rightarrow 4d^9 5s^1)$ of 18.1 kcal/mol. This is an additional validation of the RECP approach for the Pd atom and is in accord with previous studies using the MWB28 RECP.[55]

4.B.2. Basis Set Effects. We will next discuss the effect of basis sets on D_e(Pd−CO), $D_e(Pd_2)$, and $D_e(Pd_2-CO)$. We use the relative magnitude of the counterpoise correction as an indicator of the reliability of the basis set. The counterpoise-corrected bond energies are calculated as[115]

$$D_e(A-B)/cp = [E^a(A)_A - E^a(A)_{A\cdot B}] + [E^b(B)_B - E^b(B)_{A\cdot B}] - [E^{a\cup b}(A\cdot B)_{A\cdot B} - E^{a\cup b}(A)_{A\cdot B} - E^{a\cup b}(B)_{A\cdot B}] \quad (1)$$

where $D_e(A-B)/cp$ is the counterpoise-corrected bond energy of molecule AB dissociating into fragments A and B. The subscripts after the molecular species denote the geometry used, and the superscripts refer to the basis set used. For example, the subscript A·B denotes the optimum geometry of the AB complex and the subscript A denotes the optimum geometry of fragment A; furthermore, the superscript a∪b denotes the basis functions associated with fragments A and B, and the superscript a denotes basis set associated with fragment A.

The two triple-ζ basis sets (TZQ and MTZ) are considered unreliable for use with the CCSD(T) method because the counterpoise corrections for these bases are very large, especially for the small-core calculations. It can be argued that that TZQ and MTZ basis sets are not properly polarized for correlation of the $4s^24p^6$ electrons on Pd as their tighest f functions have exponents of 3.6 and 2.2, respectively, whereas the tighest f function in the MQZ basis set has an exponent of 11.4. Even if we focus on the large-core calculations where the $4s^24p^6$ electrons are not correlated, the counterpoise corrections for $D_e(Pd_2-CO)$ with the TZQ and MTZ bases are 5 and 7 kcal/mol, respectively. The largest counterpoise correction for the MQZ basis set, regardless of how many electrons are correlated, is 1.8 kcal/mol.

It is also possible to calculate the contribution of counterpoise correction for one of the two fragments by

$$D_e(\mathrm{A-B})/\mathrm{cp} = [E^a(\mathrm{A})_A - E^a(\mathrm{A})_{A\cdot B}] - [E^{a\cup b}(\mathrm{A}\cdot\mathrm{B})_{A\cdot B} - E^{a\cup b}(\mathrm{A})_{A\cdot B} - E^b(\mathrm{B})_B] \quad (2)$$

where the counterpoise correction is only applied to fragment A in eq 2. (Fragment A can be either CO or Pd_n.) A breakdown of the counterpoise corrections for PdCO and Pd_2CO is given in Table 4, where we list the total counterpoise corrections and contributions from the CO and Pd_n fragments. We can see from Table 4 that the basis set inadequacies are mainly due to the Pd basis and not the C and O basis sets. In all cases, the counterpoise corrections due to the CO fragment are less than 2 kcal/mol, whereas the counterpoise corrections on the Pd_n fragment are 1−19 kcal/mol.

4.B.3. PdCO. Turning now to Pd−CO, our results in Table 3 show that the effect of correlating the 4s and 4p electrons can be on the order of 2 kcal/mol with the MQZ basis set. The most likely explanation for the differences between the Blomberg et al.[22] and Filatov[27] results is a combination of basis set size effects and the differing numbers of correlated electrons. In light of these considerations, we take the most accurate literature results to be the values reported by Filatov.

The D_e(Pd−CO) computed with the CCSD(T)/MQZ-sc combination agrees very well with the Filatov result when counterpoise corrections are not included. The bond energies calculated with CCSD(T)/MQZ-sc and by Filatov are 43.8 and 42.8 kcal/mol, respectively. When counterpoise corrections are included, the bond energies calculated with CCSD(T)/MQZ-sc and by Filatov are 42.0 and 38.5 kcal/mol, respectively. We believe that our result is more reliable than Filatov's result because our valence electron basis set is much larger than the one used by Filatov, and it is likely that his counterpoise correction is an overestimate. Furthermore, the difference between the two calculations is significantly smaller than any of the reported relativistic effects. If our results were closer to his nonrelativistic result, then we would conclude that the RECP approach is inappropriate for PdCO, but two different RECPs give results that are consistently closer to the relativistic D_e-(Pd−CO) and r_e(Pd−CO) values. The recommended value for D_e(Pd−CO) is therefore 42.9 ± 1 kcal/mol, which is the average of 43.8 and 42.0 kcal/mol.

The bond lengths computed with the CCSD(T) correlation treatment and MQZ method also agree well with the experimental results. The CCSD(T)/MQZ-sc and experimental values for r_e(Pd−CO) are 1.834 and 1.843 Å, respectively.

4.B.4. Pd_2. The CCSD(T)/MQZ-sc value of $D_e(Pd_2)$ is 16.9 kcal/mol, which is less than the recommended[42,62] experimental value of 24 ± 4 kcal/mol. The value of 24 ± 4 kcal/mol is based on molecular parameters that were computed with nonrelativistic Hartree−Fock/configuration interaction theory. The calculation is quantitatively and qualitatively inaccurate, as the ground state used, $^1\Sigma_g^+$, is incorrect and relativistic effects are nonnegligible. In light of the problems with the experimental number, the 7 kcal/mol difference between the experimental and CCSD(T)/MQZ-sc values for $D_e(Pd_2)$ is not a major concern, and we recommend 16.9 kcal/mol as the benchmark value for Pd_2.

Another literature result worth comparing to is the MRSDCI+Q calculation of Balasubramanian,[43] where the value calculated for $D_e(Pd_2)$ is 19.8 kcal/mol. The difference between our CCSD-(T)/MQZ-sc number and the MRSDCI+Q number is 3.1 kcal/mol. We believe that the CCSD(T)/MQZ-sc number is more accurate than the other two results because we correlated more electrons and because our basis set is considerably larger. The MRSDCI+Q calculation does not include f polarization functions, and the basis set is small enough that the counterpoise correction is likely nonnegligible.

TABLE 4: Counterpoise Corrections (in kcal/mol) Given to Dissociation Energies of Pd_nCO (n = 1,2) for the Entire Molecule and for the Contributions of the Pd_n and CO Fragment

	D_e(Pd−CO)			D_e(Pd_2−CO)		
	PdCO	Pd	CO	Pd_2CO	Pd_2	CO
			Large Core[a]			
TZQ	5.49	4.19	1.30	6.91	4.97	1.94
MTZ	3.86	3.20	0.66	7.19	6.21	0.97
MQZ	0.67	0.42	0.26	1.39	0.99	0.39
			Small Core[b]			
TZQ	12.91	11.58	1.34	13.98	12.04	1.94
MTZ	12.28	11.60	0.69	19.49	18.52	0.97
MQZ	0.94	0.69	0.26	1.83	1.43	0.39

[a] The $4s^24p^6$ electrons on Pd and the $1s^2$ electrons on C and O were frozen during the correlation treatment. [b] The $1s^2$ electrons on C and O were frozen during the correlation treatment.

TABLE 5: CCSD(T) Results, the Bond Dissociation Energy, D_e, for the Dissociation of $Pd_2(^1\Sigma_g^+)$ into Ground-State Pd Atoms, the Equilibrium Bond Length, r_e, of $Pd_2(^1\Sigma_g^+)$, and the Adiabatic Transition Energy, T_e, for the $^3\Sigma_u^+ \rightarrow {}^1\Sigma_g^+$ Transition

	D_e	D_e/cp	r_e	T_e	T_e/cp
			Large Core[a]		
TZQ	10.6	5.7	2.788	−0.3	−1.4
MTZ	9.8	7.5	2.735	4.2	3.4
MQZ	8.2	7.9	2.728	3.1	3.0
			Small Core[b]		
TZQ	18.7	6.4	2.683	7.7	5.3
MTZ	16.6	8.6	2.655	10.5	8.4
MQZ	9.5	9.1	2.704	8.0	7.8

In Table 5, we present the dissociation energy for Pd_2 in the $^1\Sigma_g^+$ electronic state, along with the optimized bond lengths, r_e, for the $^1\Sigma_g^+$ state of Pd_2, and adiabatic transition energies for the $^3\Sigma_u^- \rightarrow {}^1\Sigma_g^+$ transition. We denote this quantity $T_e(^3\Sigma_u^- \rightarrow {}^1\Sigma_g^+)$.

As was discussed in section 2.C, the $^1\Sigma_g^+$ state is sometimes expected to be a van der Waals dimer. We can see from the CCSD(T)/MQZ-sc calculation that the bond energy of this state, 9.1 kcal/mol, is too strong to be considered a van der Waals interaction. For example, the bond energies of the homonuclear rare gas dimers (He, Ne, and Ar) are all less than 0.5 kcal/mol.[116] Even the Zn dimer, which is also described as a van der Waals dimer,[117] also has a well depth of less than 1 kcal/mol.[118] By comparison to these well-known van der Waals systems, we conclude that the $^1\Sigma_g^+$ state of Pd_2 is not a van der Waals dimer but is better described as a configuration interaction mixture of a van der Waals configuration and a weak σ-bond.

The most accurate $T_e(^3\Sigma_u^- \rightarrow {}^1\Sigma_g^+)$ is the counterpoise-corrected CCSD(T)/MQZ-sc calculation, where $T_e(^3\Sigma_u^- \rightarrow {}^1\Sigma_g^+) = 7.8$ kcal/mol. The value of $T_e(^3\Sigma_u^- \rightarrow {}^1\Sigma_g^+)$ is strongly influenced by the accuracy of $T_e(4d^{10}5s^0 \rightarrow 4d^95s^1)$ for the atom. The CCSD(T)/TZQ-lc calculation has the largest error in $T_e(4d^{10}5s^0 \rightarrow 4d^95s^1)$ for the atom, where the transition is overestimated by 4 kcal/mol (Table 3). Because the 5s orbitals are too high in energy, the 5s-derived σ-orbitals will also be too high in energy, which will lead to an incorrect $^3\Sigma_u^- \rightarrow {}^1\Sigma_g^+$ transition energy. We can see, consistently with this argument, that the CCSD-(T)/TZQ-lc calculation predicts the incorrect ground state for Pd_2. In fact, all of the large-core calculations have a much smaller $T_e(^3\Sigma_u^- \rightarrow {}^1\Sigma_g^+)$ value than the small-core calculations, which is consistent with the large-core calculations all overestimating $T_e(4d^{10}5s^0 \rightarrow 4d^95s^1)$ for the atom.

4.B.5. Pd_2CO. The geometries for Pd_2CO were optimized with the $4s^24p^6$ electrons uncorrelated to keep the CPU cost for a CCSD(T) geometry optimization down. On the basis of the PdCO and Pd_2 results, we can conclude that the effect of correlating the $4s^24p^6$ electrons would have affected the bond lengths by less than 0.01 Å. We assume that the most accurate value of $D_e(Pd_2-CO)$ is 69.4 ± 1 kcal/mol, which is the average of CCSD(T)/MQZ-sc and counterpoise-corrected CCSD(T)/MQZ-sc values.

Our $D_e(Pd_2-CO)$ value of 69.4 kcal/mol is in good agreement with the value not counterpoise corrected of 71.9 kcal/mol computed by Dai et al.[36] This agreement is most likely coincidental, because the basis set used by Dai et al.[36] is far to small for quantitative work, and the counterpoise corrections would be nonnegligible. For example, the CCSD(T)/TZQ calculation where the $4s^24p^6$ electrons on Pd are not correlated is the most similar to the Dai et al. calculation with respect to numbers of electrons correlated and basis set size, and the counterpoise correction for this CCSD(T) result is over 7 kcal/mol.

4.B.6. Dipole Moments. We assume that the dipole moments calculated with the CCSD(T)/MQZ-sc method are the most accurate. One interesting feature is that the dipole moments are fairly insensitive to the number of correlated electrons, as the CCSD(T)/MQZ-lc and CCSD(T)/MQZ-sc dipoles differ by 0.01−0.03 D. The most accurate dipole moments for PdCO and Pd_2CO are 2.50 and 2.81 D, respectively. Even though this paper is mainly about the energetic properties, we included the dipole moments because it was recently pointed out by Bulat et al.[119] that despite the increasing accuracy of DFT for properties such as bond energies and bond lengths, it often does poorly for dipole moments and other properties that control responses to electric fields. We hope that our CCSD(T) dipole moments will be useful as additional benchmark values for technologically important systems such as Pd_nCO.

4.C. DFT Results. DFT methods generally show smaller counterpoise corrections than WFT methods. We examined the counterpoise results for several DFT methods and found that they were less than 1 kcal/mol for the MQZ basis set and less than 2 kcal/mol for TZQ basis set. We therefore will not consider counterpoise corrections for the DFT methods.

4.C.1. Pd and Pd_2. We will begin our DFT discussion by examining how accurately DFT methods can describe $T_e(4d^{10}5s^0 \rightarrow 4d^95s^1)$. The results with the TZQ and MQZ basis sets are given in Table 6**.** In general, most of the DFT methods are within 2−5 kcal/mol of the experimental or CCSD(T)/MQZ-sc value. Including Hartree−Fock exchange lowers $T_e(4d^{10}5s^0 \rightarrow 4d^95s^1)$. For example, the $T_e(4d^{10}5s^0 \rightarrow 4d^95s^1)$ values with BLYP, B3LYP*, B3LYP, and B1LYP with the MQZ basis set are 14,9, 14.8, 14.3, and 13.3 kcal/mol, respectively, and the percentages of Hartree−Fock exchange in these methods are 0%, 15%, 20%, and 25%, respectively. We can see a similar trend by comparing local functionals to their hybrid complements; for example, the PBE and PBEh values of $T_e(4d^{10}5s^0 \rightarrow 4d^95s^1)$ are 18.9 and 17.6 kcal/mol, respectively. This trend is well understood in that Hartree−Fock theory favors high-spin states bcause it includes the Fermi hole for electrons of the same spin but not the Coulomb hole for opposite-spin electrons.

The methods with the largest errors for $T_e(4d^{10}5s^0 \rightarrow 4d^95s^1)$ are BMK and M05, where $T_e(4d^{10}5s^0 \rightarrow 4d^95s^1) = -10.1$ and 33.2 kcal/mol, respectively, with the MQZ basis set. The M05-2X functional with the MQZ basis set, which has the same functional form as M05 but a different parameter set, gives the most accurate functional with the MQZ basis set when compared with an experimental value of 21.9 kcal/mol. (The M05-2X/MQZ computed $T_e(4d^{10}5s^0 \rightarrow 4d^95s^1)$ is 19.1 kcal/mol.) However, there is significant basis set dependence for $T_e(4d^{10}5s^0 \rightarrow 4d^95s^1)$, because M05-2X is the most accurate functional with the MQZ basis set, but it is the sixth most inaccurate functional with the smaller TZQ basis set. BLYP is the most accurate DFT method for $T_e(4d^{10}5s^0 \rightarrow 4d^95s^1)$ with the TZQ basis set but is not particulary accurate with the MQZ basis set. (The BLYP/TZQ and BLYP/MQZ computed values of $T_e(4d^{10}5s^0 \rightarrow 4d^95s^1)$ are 18.9 and 14.9 kcal/mol, respectively.)

We will also discuss the Pd_2 molecule in this section so that later we will can relate the errors in the dimer to the errors in the Pd atom. The dissociation energies are reported with isolated Pd atoms in their ground states. We note that the ground states for Pd and Pd_2 predicted by each DFT method are not always correct, and we will use the ground state predicted by each method when we calculate D_e. The $T_e(4d^{10}5s^0 \rightarrow 4d^95s^1)$ values for each method are given in Table 6, so the reported D_e can easily be converted so that it corresponds to a different asymptote, if desired.

In Table 6 we have computed the dissociation energies for Pd_2 in the $^3\Sigma_u^-$ and $^1\Sigma_g^+$ electronic states with the TZQ basis set. The most notable error is that some functionals predict that the $^1\Sigma_g^+$ electronic state is lower in energy than the $^3\Sigma_u^-$ electronic state for Pd_2. The functionals that have this deficiency

TABLE 6: DFT Results, the Atomic Transition Energy, T_e, for the $4d^{10}5s^0 \rightarrow 4d^95s^1$ Transition in the Pd Atom and Dissociation Energy, D_e, and Bond Length, r_e, for Pd_2 Computed with the TZQ and MQZ Basis Sets

	TZQ					MQZ		
		$D_e(Pd_2)$		$r_e(Pd_2)$				
method	T_e[a]	$^3\Sigma_u^+$	$^1\Sigma_g^+$	$^3\Sigma_u^+$	$^1\Sigma_g^+$	T_e[a]	$D_e(Pd_2)$	$r_e(Pd_2)$
BLYP	18.91	25.8	18.2	2.527	2.749	14.92	30.8	2.500
B1LYP	16.77	16.9	9.8	2.519	2.789	13.26	21.4	2.498
B3LYP	18.06	18.6	11.4	2.512	2.768	14.31	23.1	2.488
B3LYP*	18.57	21.3	13.5	2.506	2.768	14.79	26.0	2.483
BP86	19.29	29.2	20.4	2.488	2.702	14.94	34.4	2.461
B3P86	19.27	20.7	13.2	2.475	2.720	15.59	25.4	2.453
mPWPW91	19.50	28.2	19.8	2.491	2.710	15.35	33.0	2.464
mPW1PW91	17.72	18.4	11.0	2.484	2.747	14.22	22.7	2.463
MPW1K	16.48	12.4	7.8	2.484	2.787	13.13	16.3	2.467
OLYP	25.26	13.7	10.6	2.512	2.784	20.98	16.7	2.482
O3LYP	23.78	11.4	8.2	2.502	2.794	19.73	16.3	2.476
PBE	19.52	28.8	20.5	2.491	2.708	15.74	33.8	2.464
PBEh	17.97	19.0	11.6	2.483	2.744	14.40	23.5	2.462
M05	35.72	−0.6	8.9	2.554	2.848	33.21	8.4	2.828
M05-2X	21.29	7.5	9.6	2.505	2.815	19.09	10.9	2.491
PWB6K	18.99	10.2	8.2	2.489	2.792	15.73	14.3	2.473
PW6B95	20.32	15.8	10.9	2.491	2.759	16.70	20.2	2.471
TPSS	17.56	30.0	19.6	2.482	2.710	13.54	35.2	2.456
TPSSh	16.80	25.7	15.4	2.480	2.699	13.18	30.7	2.457
B97-1	20.35	18.8	11.9	2.517	2.779	17.35	14.4	2.489
B97-2	27.53	3.3	9.8	2.503	2.773	24.00	7.4	2.475
B98	19.90	18.3	11.3	2.508	2.778	17.31	13.6	2.483
BMK[a]	−6.60	29.5	12.4	2.597	2.808	−10.07	52.0	2.578
G96LYP	18.93	24.5	16.6	2.514	2.738	14.62	29.6	2.486
mPWLYP1M	18.48	25.2	17.1	2.522	2.748	14.91	29.9	2.497
MOHLYP	26.51	2.0	3.4	2.586	2.784	22.28	6.9	2.552
XLYP	18.81	25.4	23.1	2.533	2.757	14.92	30.2	2.506

[a] A quantity of 3.15 kcal/mol was subtracted from the calculated value to account for spin−orbit coupling. [b] Calculated relative to the $4d^95s^1$ asymptote. [c] Only the results for the $^1\Sigma_g^+$ electronic state are reported for the MQZ basis set. $D_e(Pd_2)$ and $r_e(Pd_2)$ for the $^3\Sigma_u^+$ state are 2.0 kcal/mol and 2.537 Å, respectively.

are B97−2, M05, M05−2X, and MOHLYP, and these methods all overestimate $T_e(4d^{10}5s^0 \rightarrow 4d^95s^1)$ by a minimum of 2.5 kcal/mol when compared to the experimental value.

As stated earlier, M05−2X has a large error with the TZQ basis set for $T_e(4d^{10}5s^0 \rightarrow 4d^95s^1)$ but a very small error for $T_e(4d^{10}5s^0 \rightarrow 4d^95s^1)$ with the MQZ basis set. We attribute the incorrect ordering of the Pd_2 electronic states with the TZQ basis set to the error in $T_e(4d^{10}5s^0 \rightarrow 4d^95s^1)$. With the MQZ basis set, the computed $D_e(Pd_2)$ values for the $^3\Sigma_u^-$ and $^1\Sigma_g^+$ electronic states are 10.9 and 8.7 kcal/mol, respectively. We can see from this example that improvement in $T_e(4d^{10}5s^0 \rightarrow 4d^95s^1)$ leads to a correct ordering of the electronic states when the M05−2X functional is used. We do not report additional results for the $^1\Sigma_g^+$ state of Pd_2 with the MQZ basis set because the TZQ results are enough to show the relative importance of having an accurate prediction of $T_e(4d^{10}5s^0 \rightarrow 4d^95s^1)$.

The O3LYP functional with the TZQ basis set has an error greater than 2.5 kcal/mol for $T_e(4d^{10}5s^0 \rightarrow 4d^95s^1)$ but still predicts the correct ordering of the $^3\Sigma_u^-$ and $^1\Sigma_g^+$ electronic states; however, the O3LYP functional underestimates the $^3\Sigma_u^-$ to $^1\Sigma_g^+$ transition energy by 5 kcal/mol. Another consequnce of overestimating $T_e(4d^{10}5s^0 \rightarrow 4d^95s^1)$ with the TZQ basis set is an underestimation of $D_e(Pd_2)$. However, improving the basis set by using the MQZ basis set improves the $T_e(4d^{10}5s^0 \rightarrow 4d^95s^1)$ excitation energy for O3LYP substantially and significantly reduces the error for $D_e(Pd_2)$. In fact, O3LYP is the second most accurate method for $T_e(4d^{10}5s^0 \rightarrow 4d^95s^1)$ with the MQZ basis set and is the most accurate method for $D_e(Pd_2)$ with the MQZ basis set.

The final DFT functional that we discuss is BMK, which overestimates $D_e(Pd_2)$ for the $^3\Sigma_u^-$ electronic state by 22 kcal/mol with both the TZQ and the MQZ basis sets. Part of the reason for this overestimation is that BMK predicts a ground state of $4d^95s^1$ for the Pd atom. The σ-bonding orbitals in Pd_2 are derived from the 5s orbitals, which are overstabilized when the BMK functional is used. The error would be larger if we computed the error relative to the $4d^{10}5s^0$ atoms.

All of the DFT methods overestimate $r_e(Pd_2)$ with the TZQ and MQZ basis sets. We will only discuss the results with the MQZ basis set here. The most accurate method for $r_e(Pd_2)$ is B3P86 with an error of 0.036 Å and $r_e(Pd_2) = 2.453$ Å. (The accurate value of $r_e(Pd_2) = 2.417$ Å used for this test is the CCSD(T)/MQZ-sc value from Table 4.) The inclusion of Hartree−Fock exchange into the functional has a relatively small effect on $r_e(Pd_2)$. For example, compare PBE to PBEh, TPSS to TPSSh, and mPWPW to MPW1K. In all of the cases, the bond length of the local functional and its hybrid counterpart differ by less than 0.003 Å. Also, the effect of Hartree−Fock exchange on $r_e(Pd_2)$ is not always linear. For example, mPWPW, mPW1PW, and MPW1K have 0%, 25%, and 42.8% Hartree−Fock exchange, respectively, and the calculated $r_e(Pd_2)$ values for these three methods are 2.464, 2.463, and 2.467 Å, respectively. A variance in $r_e(Pd_2)$ of greater than 0.01 Å is seen in the BLYP series (BLYP, B3LYP*, B3LYP, and B1LYP). BLYP and B1LYP differ only in the percentage of Hartree−Fock exchange, and $r_e(Pd_2)$ values for these two methods are 2.500 and 2.498 Å, respectively. B3LYP, however, also scales the gradient-corrected exchange and correlation energy, and this has a much larger effect on the bond lengh, as $r_e(Pd_2) = 2.488$ Å for B3LYP, which is 0.012 Å smaller than that for BLYP. The relationship is similar with BP86 and B3P86, where $r_e(Pd_2) = 2.461$ and 2.453 Å, respectively. We can see from this that the fraction of Hartree−Fock exchange is not the parameter in the density functional to which $r_e(Pd_2)$ is most sensitive.

4.C.2. PdCO and Pd_2CO. The results for the bond energies and the dipole moments with the TZQ and MQZ basis sets are given in Table 7. We will only discuss the MQZ basis set results here. The method with the lowest error for D_e(Pd−CO) in Table 7 is PW6B95, with a value of 42.9 kcal/mol and an error of 0.1 kcal/mol. The value of $D_e(Pd_2-CO)$ computed with PW6B95 is 64.4 kcal/mol and has an error of 3.9 kcal/mol.

The method that is the most accurate for both D_e(Pd−CO) and $D_e(Pd_2-CO)$ with the MQZ basis set is O3LYP, which has errors in D_e(Pd−CO) and $D_e(Pd_2-CO)$ of 0.4 and 3.1 kcal/mol, respectively. From this we can see that the O3LYP method is very accurate for Pd systems, as it does well for $T_e(4d^{10}5s^0 \rightarrow 4d^95s^1)$, $D_e(Pd_2)$, D_e(Pd−CO), and $D_e(Pd_2-CO)$. If we were to make our recommendations entirely on energetics, O3LYP would be the preferred method.

The dipole moments are another example of how erratic the errors in DFT methods can be. The most accurate method for dipole moments is B3LYP*, which has errors in $\mu(Pd_2CO)$ and μ(PdCO) of 0.08 and 0.03 D, respectively. The performance of the B3LYP* method, as shown in Tables 7 and 8, is, however, only average for $D_e(Pd_2)$, D_e(Pd−CO), and $D_e(Pd_2-CO)$. The O3LYP method, which is accurate for bond energies, is among the more inaccurate methods for the dipole moments. O3LYP has errors in μ(PdCO) and $\mu(Pd_2CO)$ of 0.18 and 0.06 D, respectively, for an average error in the dipoles of 0.12 D. This average error of 0.12 D is the 19th highest error in dipoles of the 29 functionals tested in this paper with the MQZ basis set.

All of the DFT methods are qualitatively correct for the dipole moments in that $\mu(Pd_2CO)$ is greater in magnitude than μ(PdCO). (The CCSD(T)/MQZ-sc dipole moments for μ(PdCO) and $\mu(Pd_2CO)$ are 2.49 and 2.81 D, respectively.) The hybrid methods, in general, overestimate both μ(PdCO) and $\mu(Pd_2CO)$, whereas the local methods overestimate μ(PdCO) and underestimate $\mu(Pd_2CO)$. For example, the errors in μ(PdCO) and $\mu(Pd_2CO)$ for PBE are +0.07 and −0.16 D, respectively, and the errors in μ(PdCO) and $\mu(Pd_2CO)$ for PBEh are 0.16 and 0.10 D, respertively. Similar trends can be seen with all of the hybrid/local complements. We conclude that including Hartree−Fock exchange into the exchange functional, in general, introduces a systematic error with respect to the dipole moments.

The bonds lengths for PdCO and Pd_2CO are given in Table 8. The most accurate method for the bond lengths is TPSSh, which has a mean unsigned error of 0.01 Å when tested against r_e(Pd−CO), r_e(PdC−O), r_e(Pd−PdCO), $r_e(Pd_2-CO)$, and $r_e(Pd_2C-O)$. The most inaccurate method is M05, which has a mean unsigned error of 0.04 Å when tested against the same set of bond lengths. In general, the methods with a modest amount of Hartree−Fock exchange, i.e., 10−25%, do well for the bond lengths. For example, the mean unsigned errors in bond lengths for mPWPW91, mPW1PW91, and MPW1K are 0.017, 0.013, and 0.019 Å, respectively. We can see from mPWPW series that the average errors in r_e(Pd−CO), r_e(PdC−O), r_e(Pd−PdCO), $r_e(Pd_2-CO)$, and $r_e(Pd_2C-O)$ change by 0.01 Å as the percentage of Hartree−Fock exchange is varied. However, the two bond lengths that are the most sensitive to the percentage of Hartree−Fock exchange are r_e(PdC−O) and $r_e(Pd_2C-O)$. The mean unsigned errors for mPWPW, mPW1PW, and MPW1K when tested against r_e(PdC−O) and $r_e(Pd_2C-O)$ are 0.011, 0.007, and 0.019 Å, respectively; additionally, the average signed errors for mPWPW91, mPW1PW, and MPW1K when tested against r_e(PdC−O) and $r_e(Pd_2C-O)$ are 0.011, −0.007,

TABLE 7: DFT Results, the Bond Energies of PdCO and Pd_2CO in kcal/mol and Dipole Moments for PdCO and Pd_2CO in D with the TZQ and MQZ Basis Sets

	TZQ				MQZ			
	D_e(Pd−CO)	D_e(Pd_2−CO)	μ(PdCO)	μ(Pd_2CO)	D_e(Pd−CO)	D_e(Pd_2−CO)	μ(PdCO)	μ(Pd_2CO)
BLYP	47.6	66.2	2.60	2.69	51.2	67.1	2.51	2.61
B1LYP	38.4	56.6	2.67	2.95	41.1	56.6	2.59	2.87
B3LYP	41.2	60.6	2.67	2.91	44.1	60.8	2.59	2.83
B3LYP*	44.5	64.6	2.66	2.87	47.6	65.1	2.57	2.78
BP86	54.1	76.4	2.61	2.70	57.7	77.5	2.51	2.61
B3P86	46.7	70.3	2.70	2.94	49.7	70.7	2.61	2.86
mPWPW91	53.8	76.9	2.68	2.76	57.2	77.9	2.57	2.66
mPW1PW91	43.9	67.2	2.75	3.00	46.6	67.2	2.66	2.92
MPW1K	38.0	61.4	2.77	3.12	40.1	60.8	2.69	2.66
OLYP	43.4	68.9	2.73	2.84	47.1	72.2	2.65	2.77
O3LYP	40.4	65.6	2.74	2.94	43.7	66.3	2.67	2.87
PBE	55.2	79.2	2.65	2.73	58.8	80.4	2.56	2.65
PBEh	45.1	69.0	2.73	2.98	47.9	69.3	2.65	2.91
M05	34.4	58.5[a]	2.80	2.98	35.8	61.5[a]	2.63	2.93
M05-2X	32.2	56.2[a]	2.56	3.02	34.1	58.0	2.49	2.93
PWB6K	35.5	60.3	2.72	3.08	37.6	59.7	2.65	3.01
PW6B95	40.2	64.4	2.70	2.97	42.9	64.4	2.62	2.88
TPSS	52.7	74.7	2.83	2.86	56.1	75.4	2.73	2.78
TPSSh	48.6	70.6	2.84	2.96	51.8	71.0	2.75	2.88
B97-1	43.1	65.2	2.73	2.96	45.9	74.5	2.65	2.88
B97-2	41.0	68.6	2.73	2.98	43.8	76.5	2.65	2.89
B98	42.4	64.0	2.73	2.98	45.2	73.4	2.65	2.90
BMK	37.6[b]	38.2	2.75	3.08	38.2[b]	39.9	2.64	2.87
G96LYP	46.9	65.8	2.60	2.72	50.6	66.9	2.51	2.63
mPWLYP1M	47.1	65.9	2.63	2.76	50.3	66.6	2.54	2.67
MOHLYP	28.8	49.2[a]	2.78	2.90	39.8	59.0	2.71	2.83
XLYP	46.7	64.7	2.61	2.70	50.2	65.6	2.51	2.61

[a] The dissociation products are CO and $Pd_2(^1\Sigma_g^+)$. [b] The dissociation products are CO and $Pd(4d^95s^1)$.

and −0.019 Å, respectively. The effect of Hartree−Fock exchange on r_e(PdC−O) and r_e(Pd_2C−O) is clear from the mPWPW91 series and is a general result. All of the local methods tested in this paper as well as the hybrid mehods with less than 15% Hartree−Fock exchange (TPSSh and O3LYP) overestimate r_e(PdC−O) and r_e(Pd_2C−O), and the remaining hybrid methods underestimate r_e(PdC−O) and r_e(Pd_2C−O). B3LYP* is the most accurate for r_e(PdC−O) and r_e(Pd_2C−O), with a mean unsigned error of 0.001 Å. The B3LYP* functional also has 15% Hartree−Fock exchange energy, which appears to be a practically successful amount for the r_e(PdC−O) and r_e(Pd_2C−O) bonds. We will return to the issue of r_e(PdC−O) and r_e(Pd_2C−O) in section 4.D.

4.C.3. Total Error for the Density Functional Theory Methods. In the previous sections, we have discussed how well DFT methods can predict the energies, dipole moments, and geometries of Pd, Pd_2, PdCO, and Pd_2CO. We identified the most accurate functional for each of the different molecules, but no one functional is consistently accurate for all of the properties. We will therefore consider four quantities, mean unsigned error in bond energies, mean unsigned error in dipoles, mean unsigned error in geometries, and a quantity called the mean percent unsigned error, M%UE, which is defined as

$$\mathrm{M\%UE} = \frac{100}{m}\sum_{i=1}^{m}\frac{|x_{\mathrm{DFT}}^{(i)} - x_{\mathrm{acc}}^{(i)}|}{x_{\mathrm{acc}}^{(i)}} \qquad (3)$$

where $x_{\mathrm{DFT}}^{(i)}$ is a DFT calculated property and $x_{\mathrm{acc}}^{(i)}$ is the accurate property that is taken from experiment, when a good experiment is available, or calculated with CCSD(T)/MQZ-sc. (For D_e we average the values calculated with and without counterpoise corrections.) The properties that we consider are D_e(Pd−CO), D_e(Pd_2), D_e(Pd_2−CO), μ(PdCO), μ(Pd_2CO), r_e(Pd−CO), r_e(PdC−O), r_e(Pd_2), r_e(Pd−PdCO), and r_e(Pd_2C−O). We are not including the adiabatic transition energies in this error assessment. We could have alternatively included $T_e(4d^{10}5s^0 \rightarrow 4d^95s^1)$ in our M%UE calculation, but this would be somewhat redundant because substantial errors in $T_e(4d^{10}5s^0 \rightarrow 4d^95s^1)$ are reflected in D_e(Pd_2). We denote the mean unsigned error in bond energies, dipoles, and geometries as MUE(D_e), MUE(μ), and MUE(r_e), respectively. We report MUE(D_e), MUE(μ), MUE(r_e), and M%UE in Table 9.

The most accurate methods for bond energies, dipoles, and geometries are O3LYP, B3LYP*, and TPSSh, respectively. The method with the lowest overall M%UE is O3LYP, where M%UE = 2.3%. O3LYP is therefore our recommended method for studying Pd_nCO systems. In general, we can see that the OptX exchange functional is very accurate for the systems examined in this paper. The second most accurate method is OLYP, with a M%UE = 2.9%. If we were to focus on the TZQ basis set instead of the MQZ basis set, then the most accurate method is OLYP with M%UE = 3.8%. Another pleasing aspect of the performance of the O3LYP and OLYP functionals is that their overall errors decrease as the basis set becomes larger. For example, the M%UE values of O3LYP with the TZQ and MQZ basis sets are 6.2% and 2.3%. In contrast some methods have a low error for the TZQ basis set, but they have a noticeably larger error with the MQZ basis set. For example, the M%UE values for PBEh with the TZQ and MQZ basis sets are 3.3% and 5.6%, respectively.

TABLE 8: Bond Lengths, r_e, for PdCO and Pd_2CO, Given in Å, for a Variety of DFT Methods with the TZQ and MQZ Basis Sets

	TZQ					MQZ				
	r_e(Pd−CO)	r_e(PdC−O)	r_e(Pd−PdCO)	r_e(Pd_2−CO)	r_e(Pd_2C−O)	r_e(Pd−CO)	r_e(PdC−O)	r_e(Pd−PdCO)	r_e(Pd_2−CO)	r_e(Pd_2C−O)
BLYP	1.861	1.156	2.657	1.954	1.180	1.838	1.155	2.624	1.181	1.936
B1LYP	1.877	1.138	2.669	1.955	1.160	1.854	1.137	2.637	1.160	1.936
B3LYP	1.869	1.140	2.659	1.950	1.163	1.846	1.140	2.627	1.163	1.931
B3LYP*	1.861	1.143	2.648	1.944	1.167	1.838	1.143	2.617	1.167	1.926
BP86	1.839	1.156	2.615	1.930	1.181	1.817	1.156	2.584	1.181	1.913
B3P86	1.847	1.140	2.619	1.926	1.163	1.825	1.139	2.589	1.163	1.908
mPWPW91	1.838	1.155	2.617	1.929	1.180	1.817	1.154	2.586	1.180	1.912
mPW1PW91	1.852	1.137	2.628	1.929	1.160	1.830	1.137	2.597	1.161	1.911
MPW1K	1.864	1.127	2.637	1.932	1.148	1.842	1.126	2.608	1.149	1.913
OLYP	1.841	1.155	2.643	1.926	1.180	1.817	1.155	2.608	1.180	1.908
O3LYP	1.847	1.146	2.645	1.927	1.170	1.824	1.146	2.611	1.170	1.909
PBE	1.836	1.156	2.616	1.926	1.181	1.814	1.155	2.584	1.181	1.909
PBEh	1.849	1.138	2.626	1.926	1.161	1.827	1.138	2.595	1.162	1.908
M05	1.900	1.141	2.685	1.972	1.162	1.875	1.140	2.654	1.161	1.952
M05-2X	1.891	1.130	2.717	1.944	1.151	1.863	1.129	2.686	1.152	1.921
PWB6K	1.876	1.124	2.631	1.941	1.145	1.853	1.124	2.602	1.145	1.921
PW6B96	1.866	1.135	2.625	1.941	1.157	1.843	1.134	2.595	1.157	1.921
TPSS	1.846	1.154	2.596	1.934	1.179	1.823	1.154	2.564	1.180	1.916
TPSSh	1.851	1.147	2.602	1.933	1.171	1.828	1.147	2.570	1.172	1.915
B97-1	1.861	1.143	2.650	1.940	1.166	1.839	1.142	2.618	1.166	1.922
B97-2	1.855	1.139	2.641	1.933	1.162	1.832	1.139	2.609	1.162	1.914
B98	1.861	1.141	2.649	1.939	1.164	1.839	1.140	2.617	1.164	1.921
BMK	1.863	1.134	2.619	1.925	1.160	1.845	1.134	2.593	1.161	1.910
G96LYP	1.855	1.155	2.642	1.947	1.179	1.831	1.154	2.610	1.179	1.929
mPWLYP1M	1.863	1.151	2.658	1.952	1.175	1.840	1.151	2.625	1.176	1.934
MOHLYP	1.874	1.160	2.720	1.960	1.185	1.848	1.160	2.679	1.186	1.939
XLYP	1.861	1.156	2.667	1.958	1.180	1.843	1.155	2.633	1.181	1.940

A final comment on the M%UE values is that the hybrid methods are more accurate than the local methods. For example, compare the M%UEs of BLYP and B3LYP, PBE and PBEh, and mPWPW and mPW1PW, etc. The hybrid method with the largest M%UE is BMK, which has a M%UE of 24.7%. The reason for this large error is the large error in $D_e(Pd_2)$, which has been discussed above.

4.D. Bonding Mechanism. An interesting issue is how well small model systems like PdCO and Pd_2CO can model the bulk material, i.e., CO adsorption onto a bulk Pd surface. The experimentally preferred site of CO adsorption on a Pd(111) surface is a 3-fold hexagonal close packed site, and the experimental binding energy for this site is 35 kcal/mol.[120] The experimentally preferred site of CO adsorption on a Pd(100) surface is the bridge site, with a binding energy of 39 kcal/mol.[121] These experimental values include zero-point effects, which may alter the bond energies by ~1 kcal/mol. The systems that we have studied in this paper, PdCO and Pd_2CO, represent zero-order models of on-top and bridge sites, and our model systems cannot distinguish sites on a Pd(111) from those on a Pd(100) surface.

Since the bridge site is favored on a Pd(100) surface and a hollow site is peferred on a Pd(111) surface, we conclude that the metal structure strongly influences the CO adsorption strengths. We cannot incorporate these effects in the cluster model with no more than two Pd atoms. We can also see that the CCSD(T)/MQZ-sc values for D_e(Pd−CO) and D_e(Pd_2−CO) are larger than the values for CO adsorption on either Pd(111) or Pd(100) surface. The cluster model is correct for the relative stability of on-top versus bridge sites. The on-top site is less favored than the bridge site for both the Pd(111) and the Pd-(100) surfaces,[122] and our cluster models correctly predict this because $D_e(Pd_2-CO) > D_e(Pd-CO)$.

For metal−ligand complexes such as PdCO, the bonding mechanism is referred to as the Dewer−Chatt−Duncanson mechanism.[123,124] For PdCO, the bond is formed by donation of electron density from a CO σ-orbital to an empty 5s σ-orbital on Pd and a corresponding charge transfer from a Pd 4d π-orbital into an empty CO π^*-orbital. An analysis of PdCO by Chung et al.[25] shows that the $d\pi \rightarrow \pi^*$ back-donation is the most important factor that affects the Pd−CO bond strength. This assessment agrees with other studies[125−127] that have concluded that $d\pi \rightarrow \pi^*$ back-donation is more important than σ-donation. Chung et al. also examined the bond strengths of NiCO and PtCO and found that PdCO has the weaker metal−CO bond strength, which was explained in terms of $d\pi \rightarrow \pi^*$ back-donation. On the basis of the analysis of Chung et al., the trend of decreasing back-donation is Pt > Ni > Pd, and the back-donation trend explains the decreasing M−CO bond strength trend of Pt > Ni > Pd.

The importance of π-back-donation is a general trend that is not specific to PdCO but also explains the CO adsorption trends in Pd(100) and Pd(111).[122] On the Pd(111) surface, π back-donation is greatest for the hollow site, whereas on the Pd(100) surface, π back-donation is greatest when CO adsorbs at the bridge site. For both the Pd(100) and the Pd(111) surfaces, the on-top site has less π-back-donation than the bridge sites.

An indirect measure of the degree of back-donation is provided by examining the difference in the CO bond length between free CO and $r_e(Pd_nC-O)$. The bond length of CO is 1.128 Å, and r_e(PdC−O) is 1.138 Å; therefore π-back-donation lengthens the CO bond by 0.010 Å. We denote this CO bond

TABLE 9: Mean Unsigned Error for Dissociation Energies, Dipoles, and Bond Lengths, Denoted, MUE(D_e), MUE(μ), and MUE(r_e), Respectively, and the %MUE[a]

	TZQ				MQZ			
method	MUE(D_e)	MUE(μ)	MUE(r_e)	%MUE	MUE(D_e)	MUE(μ)	MUE(r_e)	%MUE
BLYP	5.40	0.11	0.05	7.8	7.9	0.11	0.03	10.6
B1LYP	5.96	0.16	0.05	5.0	6.4	0.08	0.03	5.6
B3LYP	4.10	0.14	0.04	4.3	5.1	0.06	0.03	5.4
B3LYP*	3.38	0.11	0.04	4.7	5.8	0.05	0.02	7.0
BP86	9.93	0.11	0.02	11.0	13.2	0.11	0.01	14.3
B3P86	2.60	0.17	0.02	4.3	5.3	0.08	0.01	6.8
mPWPW91	9.69	0.12	0.03	10.6	12.7	0.11	0.02	13.6
mPW1PW91	1.36	0.22	0.03	3.2	3.6	0.14	0.01	5.2
MPW1K	6.04	0.29	0.03	7.6	4.2	0.17	0.02	4.0
OLYP	1.37	0.13	0.03	3.8	2.4	0.10	0.02	2.9
O3LYP	4.18	0.19	0.03	6.2	1.5	0.12	0.02	2.3
PBE	11.07	0.12	0.02	11.4	14.4	0.12	0.02	14.8
PBEh	1.32	0.20	0.02	3.3	3.7	0.13	0.01	5.6
M05	9.39	0.24	0.06	12.0	8.1	0.13	0.05	10.4
M05-2X	10.64	0.14	0.06	11.6	9.0	0.06	0.04	8.2
PWB6K	7.96	0.25	0.04	9.3	6.1	0.18	0.02	5.9
PW6B95	3.17	0.18	0.03	4.1	2.8	0.10	0.02	3.4
TPSS	9.14	0.19	0.02	11.4	12.2	0.13	0.02	14.4
TPSSh	5.01	0.25	0.02	8.0	7.9	0.16	0.01	10.6
B97-1	1.99	0.19	0.04	3.6	3.5	0.11	0.02	4.0
B97-2	3.25	0.20	0.03	7.5	5.8	0.12	0.02	7.5
B98	2.47	0.20	0.04	3.7	3.2	0.12	0.02	4.1
BMK	19.56	0.27	0.05	19.7	18.8	0.10	0.03	17.9
G96LYP	4.83	0.10	0.04	6.8	7.3	0.10	0.02	9.7
mPWLYP1M	5.11	0.09	0.04	7.3	7.5	0.09	0.03	9.9
MOHLYP	16.14	0.19	0.07	17.5	8.1	0.12	0.05	9.7
XLYP	5.46	0.11	0.05	7.7	7.9	0.11	0.03	10.4

[a] The units for MUE(D_e), MUE(μ), and MUE(r_e) are kcal/mol, D, and Å, respectively, and %MUE is unitless.

lengthening as Δr_e. The CCSD(T)/MQZ-sc calculations for PdCO predict $\Delta r_e = 0.012$ Å, which is in good agreement with experiment. An important point is that the CCSD(T)/MQZ-lc value for Δr_e is also 0.012 Å, and this is worth mentioning because the geometries for Pd_2CO were optimized with CCSD(T)/MQZ-lc. The CCSD(T)/MQZ-lc geometries for Pd_2CO yield $\Delta r_e = 0.036$ Å, which indicates significantly more π-back-donation in the Pd_2CO system. This different π-back-donation between PdCO and Pd_2CO is consistent with the bulk surfaces, and we can see that the small model systems are able to qualitatively predict this difference in π-back-donation between on-top and bridge sites.

We will now discuss how well DFT can predict Δr_e. The methods that are the most accurate for Δr_e are MPW1K and M05-2X, with a mean unsigned error of 0.002 Å for both methods. It is worth pointing out that these two methods also have the highest percentage of Hartree−Fock exchange of all the DFT methods tested. The error in Δr_e seems to depend almost entirely on the percentage of Hartree−Fock exchange. For example, the mean unsigned errors in Δr_e are 0.017, 0.010, 0.007, and 0.005 Å for BLYP, B3LYP*, B3LYP, and B1LYP, respectively, where the percentages of Hartree−Fock exchange in these methods are 0%, 15%, 20%, and 25%, respectively.

The error in our recommended method, O3LYP, is 0.011 Å and is not exceptionally large. We could most likely reduce the error by increasing the fraction of Hartree−Fock exchange in O3LYP, but reoptimizing this parameter would change all of the other results and is beyond our scope. The errors for all of the local methods are in the range of 0.016−0.018 Å. Also, the methods with a high fraction of Hartree−Fock exchange do not do exceptionally well for r_e(PdC−O) or r_e(Pd_2C−O), as pointed out in section 4.C.2. It would seem that high fractions of Hartree−Fock exchange are required for semiquantitative determination of charge transfer, but a smaller fraction is required for an accurate prediction of the quantitive properties of Pd_2, PdCO, and Pd_2CO that we included in the calculation of M%UE.

It is not surprising that the hybrid DFT methods outperform local methods for these systems because a known deficiency of local functionals is their inability to accurately model charge-transfer states.[94b,128] An additional, and perhaps a very reasonable, explanation for the superiority of hybrid functionals has to do with the differences in electronic structure predicted by the various functionals. In particular, we are interested in the orbital energies of dπ electrons on the Pd_n center and the π* orbital on the CO center. The bond strength is limited by the amount of back-donation, which is in turn limited by the ability of the Pd_n center to donate electron density into the π* orbital of CO. As a consequence, the amount of back-donation will be overestimated if the π* orbitals are too low in energy. These explanations are related because one way to understand the errors in charge transfer complexes is that the orbital energy of unoccupied molecular orbitals is too low.

The incorrect description CO adsorption onto periodic metal surfaces by local functionals also has been traced back to an incorrect description of the π* orbital on CO.[122] Here we wish to further examine the same question when CO is bonded to small metal clusters and by studying the effect of including Hartree−Fock exchange in the density functional. As a first approximation, we will examine the orbital energies for the dπ orbital of isolated Pd and the HOMO, σ, and LUMO, π*, orbitals of CO with selected density functionals. These values

TABLE 10: Orbital Energies, in E_h, for the dπ Orbital of an Isolated Pd Atom and the HOMO and LUMO of an Isolated CO Fragment and the Energy Difference between the dπ Orbital of Pd and the LUMO of CO, in kcal/mol

	% Hartree−Fock	Pd/dπ	CO/HOMO	CO/LUMO	ΔE(LUMO − dπ)
BLYP	0	−0.147	−0.332	−0.074	45.7
B3LYP*	15	−0.183	−0.373	−0.049	83.5
B3LYP	20	−0.193	−0.387	−0.040	95.8
B1LYP	25	−0.197	−0.393	−0.026	107.7
mPWPW91	0	−0.150	−0.335	−0.077	45.9
mPW1PW91	25	−0.199	−0.396	−0.027	107.5
MPW1K	42.8	−0.236	−0.440	0.004	150.6
OLYP	0	−0.142	−0.330	−0.071	44.1
O3LYP	11.6	−0.168	−0.362	−0.051	73.5

are given in Table 10 for the BLYP, mPWPW, and the OLYP series.

We can see that all of the local methods have a smaller HOMO−LUMO gap in CO than the hybrid methods. We also note that the HOMO−LUMO gap increases as the percentage of Hartree−Fock exchange increases. This agrees with the previously known[129] result that conventional local exchange functionals, such as Becke88,[47] underestimate HOMO−LUMO gaps and Hartree−Fock exchange alone will overestimate gaps. The underestimation of the energy of the LUMO on CO by local methods could be balanced by a corresponding underestimation of the energy of the dπ orbitals on Pd. But, we can see that the dπ eigenvalues decrease as the percentage of Hartree−Fock exchange energy is increased, which would only exacerbate the problem.

The final quantity in Table 10 that we will examine is denoted ΔE(LUMO − dπ) and is the difference in energy of the LUMO on an isolated CO and the dπ orbital of an isolated Pd atom. From Table 8 we can see that ΔE(LUMO − dπ) linearly increases with the percentage of Hartree−Fock exchange for the BLYP series and the mPWPW91 series. The ΔE(LUMO − dπ) quantity, to a first approximation, explains the overestimation of bond strengths and π-back-donation by the local functionals and why the bond strengths and π-back-donation decrease as the percentage of Hartree−Fock exchange is increased.

5. Conclusion

Systems such as Pd_2, PdCO, and Pd_2CO are very challenging from a theoretical standpoint because of large electron-correlation and relativistic effects. Relativistic effective core potentials are often used to reduce the number of explicitly correlated electrons and to implicitly treat the relativistic effects. A primary relativistic effect that the RECPs are tested against is the adiabatic transition energy for the Pd atom, $T_e(4d^{10}5s^0 \rightarrow 4d^9 5s^1)$. This quantity is relevant for a large number of bonding situations, including the Pd−Pd bond in Pd_2. A recent paper[27] has pointed out the larger relativistic effect in PdCO, where the strong Pd−CO bond is explained in terms of a Dewer−Chatt−Duncanson charge-transfer mechanism. For this case, the $T_e(4d^{10}5s^0 \rightarrow 4d^9 5s^1)$ value is not very important. In this paper we have justified the use of relativistic core potentials for charge-transfer systems such as PdCO.

Prior to this study, it might have been tempting to use local DFT methods to study the interaction of CO and Pd_n fragments, because it is well-known[90,130−140] that static correlation can degrade the quality of hybrid DFT calculations. In this work, we have examined the role of static correlation for Pd, Pd_2, PdCO, and Pd_2CO and by computing $T_e(4d^{10}5s^0 \rightarrow 4d^9 5s^1)$, $D_e(Pd_2)$, D_e(PdCO), and $D_e(Pd_2CO)$ values using the CCSD(T) level of electron correlation with different sets of reference orbitals, i.e., Hartree−Fock orbitals and Kohn−Sham orbitals. The three bond energies were insensitive to the choice of reference orbitals, and from this we concluded that Pd, Pd_2, PdCO, and Pd_2CO can be treated using single-reference methods. We have computed a set of properties using CCSD(T) and a large basis set that we believe represents a decisive set of data for testing more approximate methods, such as density functional theory. The properties that we have computed are the bond energies and bond lengths of Pd_2, PdCO, and Pd_2CO and the dipole moments of PdCO and Pd_2CO. Using this database, we have determined that the hybrid O3LYP functional performs the best (out of 27 functionals tested) when evaluated over this broad data set.

We have also diagnosed some of the reasons for the deficiencies of DFT for the Pd_2, PdCO, and Pd_2CO systems. In particular, the accuracy of the Pd_2 bond strength is very sensitive to the accuracy of the $T_e(4d^{10}5s^0 \rightarrow 4d^9 5s^1)$ transition in the Pd atom, because the Pd_2 bonding σ-orbitals are derived from the 5s orbital of Pd. We have shown that the DFT methods that have large errors for $T_e(4d^{10}5s^0 \rightarrow 4d^9 5s^1)$ also have large errors for $D_e(Pd_2)$. Another problem that some DFT methods have is an overestimation of the HOMO−LUMO gap for CO. This overestimation leads to an overestimation of π-back-donation in the Pd_n−CO bond. The end result of too much π-back-donation is a Pd_n−CO bond strength that is much too high. We have seen that the hybrid methods have larger HOMO−LUMO gaps than the local methods and are therefore more accurate than the local methods for the Pd_n−CO bond strengths.

Acknowledgment. We gratefully acknowledge Mark Iron and Yan Zhao for assistance. This work is supported in part by the Defense−University Research Initiative in Nanotechnology (DURINT) of the U. S. Army Research Laboratory and the U. S. Army Research Office under agreement number DAAD-190110503, by the National Science Foundation under grant number CHE-0203346, and by the Office of Naval Research under award number N00014-05-1-0538.

Supporting Information Available: CASPT2 calculations for Pd_2 and properties for Pd_2 calculated with the MQZ basis set. This information is available free of charge via the Internet at http://pubs.acs.org.

References and Notes

(1) Gasteiger, H. A.; Kocha, S. S.; Sompalli, B.; Wagner, F. T. *Appl. Catal., B* **2005**, *56*, 9.

(2) Maillared, F.; Lu, G.-Q.; Wiecowski, A.; Stimming, U. *J. Phys. Chem. B* **2005**, *109*, 16230.

(3) Ioroi, T.; Yasuda, K. J. *Electrochem. Soc.* **2005**, *152*, A1917.

(4) Léger, J.-M.; Rousseau, S.; Coutanceau, C.; Hahn, F.; Lamy, C. *Electrochim. Acta* **2005**, *50*, 5118.

(5) Carrette, L.; Friedrich, K. A.; Stimming, U. *Chem. Phys. Chem.* **2000**, *1*, 162.

(6) Adams, W. A.; Blair, J.; Bullock, K. R.; Gardner, C. L. *J. Power Sources* **2005**, *145*, 55.
(7) Zhou, W. J.; Li, W. Z.; Song, S. Q.; Zhou, Z. H.; Jiang, L. H.; Sun, G. O.; Xin, X. Q.; Pouliantis, K.; Kantou, S.; Tsiakara, P. *J. Power Sources* **2004**, *131*, 217.
(8) Li, X.; Hsing, I.-M. *Electrochim. Acta* **2006**, *51*, 3477.
(9) Coutanceau, C.; Demarconnay, L.; Lamy, C.; Léger, J.-M. *J. Power Sources* **2006**, *156*, 14.
(10) Kotobuki, M.; Watanabe, A.; Uchida, H.; Yamashita, H.; Watanabe, M. *J. Catal.* **2005**, *236*, 262.
(11) Molnar, A.; Sarkany, A.; Varga, M. *J. Mol. Catal. A: Chem* **2001**, *173*, 185.
(12) Braunstein, P. *J. Organomet. Chem.* **2004**, *689*, 3953.
(13) Szymanska-Buzar, T. *Coord. Chem. Rev.* **2006**, *250*, 976.
(14) Kimmich, B. F. M.; Fagan, P. J.; Hauptman, E.; Marshall, W. J.; Bullock, R. M. *Organometallics* **2005**, *24*, 6220.
(15) Raghavachari, K.; Anderson, J. B. *J. Phys. Chem.* **1996**, *100*, 12960.
(16) Roos, B. O. In *Theory and Applications of Computational Chemisty: The First Forty Years*; Dykstra, C., Frenking, G., Kim, K. S., Scuseria, G. E., Eds.; Elsevier: Amsterdam, 2005; p 725.
(17) Chong, D. P.; Langhoff, S. R. *J. Chem. Phys.* **1986**, *84*, 5606.
(18) Čížek, J. *Adv. Chem. Phys.* **1969**, *14*, 35.
(19) Purvis, G. D.; Bartlett, R. J. *J. Chem. Phys.* **1982**, *76*, 1910.
(20) Raghavachari, K.; Trucks, G. W.; Pople, J. A.; Head-Gordon, M. *Chem. Phys. Lett.* **1996**, *157*, 479.
(21) McMichael, R. C.; Hay, J. P. *J. Chem. Phys.* **1985**, *83*, 4641.
(22) Blomberg, M. R. A.; Lebrilla, C. B.; Siegbahn, P. E. M. *Chem. Phys. Lett.* **1988**, *150*, 522.
(23) Chung, S.-C.; Krueger, S.; Pacchioni, G.; Roesch, N. *J. Chem. Phys.* **1995**, *102*, 3695.
(24) Frankcombe, K.; Cavell, K. J.; Yates, B. F.; Knott, R. B. *J. Phys. Chem.* **1995**, *99*, 14316.
(25) Chung, S.-C.; Krueger, S.; Ruzankin, S. P.; Pacchioni, G.; Roesch, N. *Chem. Phys. Lett.* **1996**, *248*, 109.
(26) Tremblay, B.; Manceron, L. *Chem. Phys.* **1999**, *250*, 187.
(27) Filatov, M. *Chem. Phys. Lett.* **2003**, *373*, 131.
(28) Wu, Z. J.; Li, H. J.; Meng, J. *J. Phys. Chem. A* **2004**, *108*, 10906.
(29) Nava, P.; Sierka, M.; Ahlrichs, R. *Phys. Chem. Chem. Phys.* **2004**, *6*, 5338.
(30) Pacchioni, G.; Koutecky, J.; Fantucci, P. *Chem. Phys. Lett.* **1982**, *92*, 486.
(31) Pacchioni, G.; Koutecky, J. *J. Phys. Chem.* **1987**, *91*, 2658.
(32) Manceron, L.; Tremblay, B.; Alikhani, M. E. *J. Phys. Chem. A* **2000**, *104*, 3750.
(33) Walker, N. R.; Hui, J. K.-H.; Gerry, M. C. L. *J. Phys. Chem. A* **2002**, *106*, 5803.
(34) Krauss, M.; Stevens, W. J. *Annu. Rev. Phys. Chem.* **1984**, *35*, 357.
(35) Schwerdtfeger, P.; McFeaters, J. S.; Moore, J. J.; McPherson, D. M.; Cooney, R. P.; Bowmaker, G. A.; Dolg, M.; Andrae, D. *Langmuir* **1991**, *7*, 116.
(36) Dai, D.; Roszak, S.; Balasubramanian. *J. Phys. Chem.* **1996**, *100*, 1471.
(37) Rochefort, A.; Fournier, R. *J. Phys. Chem.* **1996**, *100*, 13506.
(38) Schultz, N. E.; Zhao, Y.; Truhlar, D. G. *J. Phys. Chem. A* **2005**, *109*, 4388.
(39) Schultz, N. E.; Zhao, Y.; Truhlar, D. G. *J. Phys. Chem. A* **2005**, *109*, 11127.
(40) Kohn, W.; Becke, A. D.; Parr, R. G. *J. Phys. Chem.* **1996**, *100*, 12974.
(41) Moore, C. E. *Atomic Energy Levels*; National Bureau of Standards, U. S. Government Printing Office: Washington, DC, 1949; Vol. I−III.
(42) Morse, M. D. *Chemical Bonding In The Late Transition Metals: The Nickel and Copper Group Dimers*; JAI Press: Greenwich, CT, 1993; Vol. 1.
(43) Balasubramanian, K. *J. Chem. Phys.* **1988**, *89*, 6310.
(44) Bauschlicher, C. W. J. *Chem. Phys. Lett.* **1982**, *91*, 4.
(45) Xiao, C.; Krüger, S.; Belling, T.; Mayer, M.; Rösch, N. *Int. J. Quantum Chem.* **1999**, *74*, 405.
(46) Ahlrichs, R.; Scharf, P.; Erhardt, C. *J. Chem. Phys.* **1985**, *82*, 890.
(47) Becke, A. D. *Phys. Rev. A* **1988**, *38*, 3098.
(48) Perdew, J. P. *Phys. Rev. B* **1986**, *33*, 8822.
(49) Bauschlicher, C. W. J.; Siegbahn, P.; Pettersson, L. G. M. *Theor. Chim. Acta* **1988**, *74*, 479.
(50) Møller, C.; Plesset, M. S. *Phys. Rev.* **1934**, *46*, 618.
(51) Hehre, W. J.; Radom, L.; Schleyer, P. v. R.; Pople, J. A. *Ab Initio Molecular Orbital Theory*; Wiley: New York, 1986.
(52) Cowan, R. D.; Griffin, D. C. *J. Opt. Soc. Am.* **1976**, *66*, 1010.
(53) Martin, R. L. *J. Phys. Chem.* **1983**, *87*, 750.
(54) Filatov, M. *Chem. Phys. Lett.* **2002**, *365*, 222.
(55) Andrae, D.; Haeussermann, U.; Dolg, M.; Stoll, H.; Preuss, H. *Theor. Chim. Acta* **1990**, *77*, 123.
(56) Hay, P. J.; Wadt, W. R. *J. Chem. Phys.* **1985**, *82*, 270.
(57) Hay, P. J.; Wadt, W. R. *J. Chem. Phys.* **1985**, *82*, 299.
(58) Slater, J. C. *Quantum Theory of Molecules and Solids*; McGraw-Hill: New York, 1974; Vol. 4.
(59) Lee, C.; Yang, W.; Parr, R. G. *Phys. Rev. B* **1988**, *37*, 785.
(60) Lin, S. S.; Strauss, B.; Kant, A. *J. Chem. Phys.* **1969**, *51*, 2282.
(61) Shim, I.; Gingerich, K. A. *J. Chem. Phys.* **1984**, *80*, 5107.
(62) Morse, M. D. *Chem. Rev.* **1986**, *86*, 1049.
(63) Ho, J.; Ervin, K. M.; Polak, M. L.; Gilles, M. K.; Lineberger, W. C. *J. Chem. Phys.* **1991**, *95*, 4845.
(64) Lombardi, J. R.; Davis, B. *Chem. Rev.* **2002**, *102*, 2431.
(65) Nakao, T.; Dixon, D. A.; Chen, H. *J. Phys. Chem.* **1993**, *97*, 12665.
(66) Harada, M.; Dexpert, H. *J. Phys. Chem.* **1996**, *100*, 565.
(67) Valerio, G.; Toulhoat, H. *J. Phys. Chem.* **1996**, *100*, 10827.
(68) Cui, Q.; Musaev, D. G.; Morokuma, K. *J. Chem. Phys.* **1998**, *108*, 8418.
(69) Nava, P.; Sierka, M.; Ahlrichs, R. *Phys. Chem. Chem. Phys.* **2003**, *5*, 3372.
(70) Yanagisawa, S.; Tsuneda, T.; Hirao, K. *J. Comput. Chem.* **2001**, *22*, 1995.
(71) Efremenko, I.; German, E. D.; Sheintuch, M. *J. Phys. Chem. A* **2000**, *104*, 8089.
(72) Wu, Z. J. *Chem. Phys. Lett.* **2004**, *383*, 251.
(73) Stevens, W. J.; Basch, H.; Krauss, M. *J. Chem. Phys.* **1984**, *81*, 6026.
(74) Stevens, W. J.; Krauss, M.; Basch, H.; Jasien, P. G. *Can. J. Chem.* **1992**, *70*, 612.
(75) Cundari, T. R.; Stevens, W. J. *J. Chem. Phys.* **1993**, *98*, 5555.
(76) Igel-Mann, G.; Stoll, H.; Preuss, H. *Mol. Phys.* **1988**, *65*, 1321.
(77) Werner, H.-J.; Knowles, P. J. *J. Chem. Phys.* **1988**, *89*, 5803.
(78) Knowles, P. J.; Werner, H.-J. *Chem. Phys. Lett.* **1988**, *145*, 514.
(79) Anderson, K.; Roos, B. *Modern Electronic Structure Theory*; World Scientific: New York, 1995.
(80) Yanagisawa, S.; Tsuneda, T.; Hirao, K. *J. Chem. Phys.* **2000**, *112*, 545.
(81) Barden, C. J.; Rienstra-Kiracofe, J. C.; Schaefer, H. F. I. *J. Chem. Phys.* **2000**, *113*, 690.
(82) Durà-Vilà, V.; Gale, J. D. *J. Phys. Chem. B* **2001**, *105*, 6158.
(83) Perdew, J. P.; Burke, K.; Ernzerhof, M. *Phys. Rev. Lett.* **1996**, *77*, 3865.
(84) Stephens, P. J.; Devlin, F. J.; Chabalowski, C. F.; Frisch, M. J. *J. Phys. Chem.* **1994**, *98*, 11623.
(85) Adamo, C.; Barone, V. *Chem. Phys. Lett.* **1997**, *274*, 242.
(86) Reiher, M.; Salomon, O.; Hess, B. A. *Theor. Chim. Acc.* **2001**, *107*, 48.
(87) Adamo, C.; Barone, V. *J. Chem. Phys.* **1998**, *108*, 664.
(88) Perdew, J. P. In *Electronic Structure of Solids '91*; Ziesche, P., Esching, H., Eds.; Akademie Verlag: Berlin, 1991; p 11.
(89) Lynch, B. J.; Fast, P. L.; Harris, M.; Truhlar, D. G. *J. Phys. Chem. A* **2000**, *104*, 4811.
(90) Handy, N. C.; Cohen, A. J. *Mol. Phys.* **2001**, *99*, 403.
(91) Hoe, W.-M.; Cohen, A. J.; Handy, N. C. *Chem. Phys. Lett.* **2001**, *341*, 319.
(92) Adamo, C.; Cossi, M.; Barone, V. *J. Mol. Struct. (THEOCHEM)* **1999**, *493*, 145.
(93) Tao, J.; Perdew, J. P.; Staroverov, V. N.; Scuseria, G. E. *Phys. Rev. Lett.* **2003**, *91*, 146401.
(94) (a) Zhao, Y.; Schultz, N. E.; Truhlar, D. G. *J. Chem. Phys.* **2005**, *123*, 116103. (b) Zhao, Y.; Schultz, N. E.; Truhlar, D. G. *J. Chem. Theory Comput.* **2006**, *2*, 364.
(95) Zhao, Y.; Truhlar, D. G. *J. Phys. Chem. A* **2005**, *109*, 5656.
(96) Schmider, H. L.; Becke, A. D. *J. Chem. Phys.* **1998**, *108*, 9624.
(97) Hamprecht, F. A.; Cohen, A. J.; Tozer, D. J.; Handy, N. C. *J. Chem. Phys.* **1998**, *109*, 6264.
(98) Wilson, P. J.; Bradley, T. J.; Tozer, D. J. *J. Chem. Phys.* **2001**, *115*, 9233.
(99) Boese, A. D.; Martin, J. M. L. *J. Chem. Phys.* **2004**, *121*, 3405.
(100) Xu, X.; Goddard, W. A. I. *Proc. Natl. Acad. Sci. U.S.A.* **2004**, *101*, 2673.
(101) Schultz, N. E.; Zhao, Y.; Truhlar, D. G. *J. Phys. Chem. A* **2005**, *109*, 11127.
(102) Gill, P. M. W. *Mol. Phys.* **1996**, *89*, 433.
(103) Werner, H.-J.; Knowles, P. J.; Schuetz, M.; Lindh, R.; Celani, P.; Korona, T.; Rauhut, G.; Manby, F. R.; Amos, R. D.; Bernhardsson, A.; Berning, A.; Cooper, D. L.; Deegan, M. J. O.; Dobbyn, A. J.; Ecker, F.; Hampel, C.; Hetzer, A.; Lloyd, W.; McNicholas, S. J.; Meyer, W.; Mura, M. E.; Nicklass, A.; Palmieri, P.; Pitzer, R.; Schumann, U.; Stoll, H.; Stone, A. J.; Tarroni, R.; Thorsteinsson, T. *Molpro*, version 2002.6; Cardiff University: Stuttgart, Germany, 2006.
(104) Frisch, M. J.; Trucks, G. W.; Schlegel, H. B.; Scuseria, G. E.; Robb, M. A.; Cheeseman, J. R.; Montgomery, J. A., Jr.; Vreven, T.; Kudin, K. N.; Burant, J. C.; Millam, J. M.; Iyengar, S. S.; Tomasi, J.; Barone, V.; Mennucci, B.; Cossi, M.; Scalmani, G.; Rega, N.; Petersson, G. A.; Nakatsuji, H.; Hada, M.; Ehara, M.; Toyota, K.; Fukuda, R.; Hasegawa, J.; Ishida, M.; Nakajima, T.; Honda, Y.; Kitao, O.; Nakai, H.; Klene, M.; Li,

X.; Knox, J. E.; Hratchian, H. P.; Cross, J. B.; Bakken, V.; Adamo, C.; Jaramillo, J.; Gomperts, R.; Stratmann, R. E.; Yazyev, O.; Austin, A. J.; Cammi, R.; Pomelli, C.; Ochterski, J. W.; Ayala, P. Y.; Morokuma, K.; Voth, G. A.; Salvador, P.; Dannenberg, J. J.; Zakrzewski, V. G.; Dapprich, S.; Daniels, A. D.; Strain, M. C.; Farkas, O.; Malick, D. K.; Rabuck, A. D.; Raghavachari, K.; Foresman, J. B.; Ortiz, J. V.; Cui, Q.; Baboul, A. G.; Clifford, S.; Cioslowski, J.; Stefanov, B. B.; Liu, G.; Liashenko, A.; Piskorz, P.; Komaromi, I.; Martin, R. L.; Fox, D. J.; Keith, T.; Al-Laham, M. A.; Peng, C. Y.; Nanayakkara, A.; Challacombe, M.; Gill, P. M. W.; Johnson, B.; Chen, W.; Wong, M. W.; Gonzalez, C.; Pople, J. A. *Gaussian 03*, revision C.01; Gaussian, Inc.: Wallingford, CT, 2003.

(105) (a) Bylaska, E. J.; de Jong, W. A.; Kowalski, K.; Straatsma, T. P.; Valiev, M.; Wang, D.; Aprà, E.; Windus, T. L.; Hirata, S.; Hackler, M. T.; Zhao, Y.; Fan, P.-D.; Harrison, R. J.; Dupuis, M.; Smith, D. M. A.; Nieplocha, J.; Tipparaju, V.; Krishnan, M.; Auer, A. A.; Nooijen, M.; Brown, E.; Cisneros, G.; Fann, G. I.; Früchtl, H.; Garza, J.; Hirao, K.; Kendall, R.; Nichols, J. A.; Tsemekhman, K.; Wolinski, K.; Anchell, J.; Bernholdt, D.; Borowski, P.; Clark, T.; Clerc, D.; Dachsel, H.; Deegan, M.; Dyall, K.; Elwood, D.; Glendening, E.; Gutowski, M.; Hess, A.; Jaffe, J.; Johnson, B.; Ju, J.; Kobayashi, R.; Kutteh, R.; Lin, Z.; Littlefield, R.; Long, X.; Meng, B.; Nakajima, T.; Niu, S.; Pollack, L.; Rosing, M.; Sandrone, G.; Stave, M.; Taylor, H.; Thomas, G.; van Lenthe, J.; Wong, A.; Zhang, Z. *NWChem, A Computational Chemistry Package for Parallel Computers*, version 5.0; Pacific Northwest National Laboratory: Richland, WA, 2006. (b) Kendall, R. A.; Apra, E.; Bernholdt, D. E.; Bylaska, E. J.; Dupuis, M.; Fann, G. I.; Harrison, R. J.; Ju, J.; Nichols, J. A.; Nieplocha, J.; Straatsma, T. P.; Windus, T. L.; Wong, A. T. *Comput. Phys. Commun.* **2000**, *128*, 260.

(106) (a) Frisch, M. J.; Pople, J. A.; Binkley, J. S. *J. Chem. Phys.* **1984** *80*, 3265. (b) Fast, P. L.; Sánchez, M. L.; Truhlar, D. G. *Chem. Phys. Lett.* **1999**, *306*, 407.

(107) Krishnan, R.; Binkley, J. S.; Seeger, R.; Pople, J. A. *J. Chem. Phys.* **1980**, *72*, 650.

(108) Quintal, M. M.; Karton, A.; Iron, M. A.; Boese, A. D.; Martin, J. M. L. *J. Phys. Chem. A* **2005**.

(109) Woon, D. E.; Dunning, T. H. J. *J. Chem. Phys.* **1993**, *98*, 1358.

(110) Balabanov, N. B.; Peterson, K. A. *J. Chem. Phys.* **2005**, *123*, 064107.

(111) Lee, T. J.; Taylor, P. R. *Int. J. Quantum Chem. Symp.* **1989**, *23*, 199.

(112) Lambert, N.; Kaltsoyannis, N.; Price, S. D.; Žabak, J.; Herman, Z. *J. Phys. Chem. A* **2006**, *110*, 2898.

(113) Villaume, S.; Daniel, C.; Strich, A.; Perera, S. A.; Bartlett, R. J. *J. Chem. Phys.* **2005**, *122*, 44313.

(114) Beran, G. J. O.; Gwaltney, S. R.; Head-Gordon, M. *Phys. Chem. Chem. Phys.* **2003**, *5*, 2488.

(115) Boys, S. F.; Bernardi, F. *Mol. Phys.* **1970**, *19*, 553.

(116) Laschuk, E. F.; Martins, M. M.; Evangelisti, S. *Int. J. Quantum Chem.* **2003**, *95*, 303.

(117) Gustev, G. L.; Bauschlicher, C. W. J. *J. Phys. Chem. A* **2003**, *107*, 4755.

(118) Czajkowski, M. A.; Koperski, J. *Spectrochim. Acta A* **1999**, *55*, 2221.

(119) Bulat, F. A.; Toro-Labbé; Champagne, B.; Kirtman, B.; Yang, W. *J. Chem. Phys.* **2005**, *123*, 014319.

(120) Conrad, H. *Surf. Sci.* **1974**, *43*, 462.

(121) Yeo, Y. Y. *J. Chem. Phys.* **1996**, *106*, 392.

(122) Mason, S. E.; Grinberg, I.; Rappe, A. M. *Phys. Rev. B* **2004**, *69*, 161401.

(123) Dewar, M. J. S. *Bull. Soc. Chim. Fr.* **1951**, *18*, 71.

(124) Chatt, J.; Duncanson, L. A. *J. Chem. Soc.* **1953**, 2939.

(125) Li, J.; Schreckenbach, G.; Ziegler, T. *J. Am. Chem. Soc.* **1995**, *117*, 486.

(126) Blomberg, M. R. A.; Brandemark, U.; Johansson, J.; Siegbahn, P. E. M.; Wennerberg, J. *J. Chem. Phys.* **1988**, *88*, 4324.

(127) Bauschlicher, C. W., Jr.; Bagus, P. S.; Nelin, C. J.; Roos, B. O. *J. Chem. Phys.* **1986**, *85*, 354.

(128) Ruiz, E.; Salahub, D. R.; Vela, A. *J. Am. Chem. Soc.* **1995**, *117*, 1141.

(129) Teale, A. M.; Tozer, D. J. *Phys. Chem. Chem. Phys.* **2005**, *7*, 2991.

(130) Slater, J. C. *Phys. Rev.* **1954**, *91*, 528.

(131) Tschinke, V.; Ziegler, T. A. *J. Chem. Phys.* **1990**, *93*, 8051.

(132) Ziegler, T. A. *Chem. Rev.* **1991**, *91*, 651.

(133) Becke, A. D. *J. Chem. Phys.* **1993**, *98*, 5648.

(134) Perdew, J. P.; Burke, K.; Ernzerhof, M. Local and Gradient-Corrected Density Functionals. In *Chemical Applications of Density-Funtional Theory*; Laird, B., Ross, R. B., Ziegler, T., Eds.; ACS Symposium Series 629; American Chemical Society: Washington, DC, 1996; pp 453−462.

(135) Gitsenko, O. V.; Schipper, P. R. T.; Baerends, E. J. *J. Chem. Phys.* **1997**, *107*, 5007.

(136) Becke, A. D. *J. Chem. Phys.* **2000**, *112*, 4020.

(137) Cohen, A. J.; Handy, N. C. *Mol. Phys.* **2001**, *99*, 607.

(138) Becke, A. D. *J. Chem. Phys.* **2003**, *119*, 2972.

(139) (a) Cramer, C. J.; Wloch, M.; Piecuch, P.; Puzzarini, C.; Gagliardi, L. *J. Phys. Chem. A* **2006**, *110*, 1991. (b) Cramer, C. J.; Kinal, A.; Wloch, M.; Piecuch, P.; Gagliardi, L. *J. Phys. Chem. A* **2006**, *110*, 11557.

(140) Rudra, I.; Wu, Q.; Voorhis, T. V. *J. Chem. Phys.* **2006**, *124*, 1.